

## **A strong influence of the mid-Pleistocene transition on the monsoon and associated productivity in the Indian Ocean**

**Sudhira R. Bhadra<sup>1,2\*</sup>, Rajeev Saraswat<sup>1</sup>**

<sup>1</sup>Micropaleontology Laboratory, Geological Oceanography Division,  
National Institute of Oceanography, Goa, India

<sup>2</sup>Centre for Earth Sciences, Indian Institute of Science, Bengaluru, India

\* For correspondence: sudhirabhadr@gmail.com

### **Abstract**

The short-term variability in the Indian monsoon is well documented through instrumental records and paleoclimatic studies of the recent geological past. However, the effect of mid-Pleistocene transition (MPT) on the Indian monsoon has not been discussed extensively due to the scarcity of long-term records of changes in monsoon strength. We have used a 1.45 myr record of planktic foraminifera assemblages from the Site U1446 to understand the effect of the MPT on monsoon and associated processes. From the variability in the abundance of the summer monsoon assemblage, it is evident that the Indian summer monsoon (ISM) was stronger during the warm interstadials and weaker during the stadials, whereas the winter monsoon assemblage suggests a weakened winter monsoon during the interstadials. From the variation in eutrophic assemblage, it is inferred that, throughout the studied interval, productivity was controlled by the ISM. We report a large-scale reorganization of the Indian monsoon system after the onset of the MPT, which resulted in the strengthening of ISM. We also report that during the post MPT period, the summer monsoon was influenced by the 23 kyr precession cycle and the 100 kyr eccentricity cycle strongly modulated the winter monsoon.

**Keywords:** Indian Monsoon, mid-Pleistocene Transition, Planktic Foraminifera, Quaternary

## 1. Introduction

The Indian monsoon is a unique seasonal reversal of the surface winds driven by the migration of the intertropical convergence zone (ITCZ) and atmospheric pressure gradients over central Asia (Wyrтки et al., 1971; Webster, 1986). During the summer monsoon season, the differential heating between the warmer Indian subcontinent and the cooler Indian Ocean induces southwesterly winds, bringing heavy precipitation throughout the Peninsular India (Krishnamurti, 1985; Gadgil, 2003). The intense heating creates a large pressure difference that shifts ITCZ to a large extent. The low pressure is driven by both the direct heating of the Indian landmass and the latent heating of the atmosphere (Webster et al., 1998; Fasullo and Webster, 2003). The southern Indian Ocean acts as the source of the latent heat and moisture caused by intense evaporation. This hot and moisture-rich wind system originating in the southern Indian Ocean deflects to its right in the Arabian Sea due to the Coriolis effect and travels to the Indian mainland and precipitates as rainfall in the Himalaya's slopes, further strengthening the low pressure (Clemens et al., 1991; Schott and McCreary, 2001; Shankar et al., 2002; Gadgil et al., 2007). Although the broad mechanism facilitating the Indian monsoon is known, its temporal variability is still a mystery, hampering robust projections.

Several modelling studies focused on the effect of radiative forcing on the Indian summer monsoon (Kitoh et al., 1997; May, 2004; Meehl and Arblaster, 2003; Ueda et al., 2006; Turner et al., 2007; Ashfaq et al., 2009; Sabade et al., 2011). The results vary, with a few projecting a decrease in the summer monsoonal rainfall due to the weakening of large-scale monsoon circulation (Ashfaq et al., 2009), while others suggest an increase in precipitation due to the enhanced moisture convergence resulting from the increase in atmospheric moisture content (Seth et al., 2013; Kitoh et al., 2013; Lee and Wang, 2014). The Indian Ocean is the primary moisture source for the summer monsoon precipitation (Meehl, 1997; Wajsowicz and Schopf, 2001). The changes in both the Northern and Southern Hemisphere insolation affect the Indian monsoon. While the insolation changes in the Northern Hemisphere have a more local and immediate effect, the Southern Hemisphere insolation changes have a remote and delayed impact (Liu et al., 2006). The uplift of the Himalayas and Tibetan plateau has also been associated with the change in Indian monsoon strength (Zhang et al., 2012; Singh and Gupta, 2014). The differential heating during the summer season lowers the pressure over the Tibetan Plateau as compared to the Indian subcontinent and strengthens the monsoon (Webster et al., 1998).

The changes in the solar radiation intensity or insolation caused by the changes in the earth's orbit, namely the Milankovitch Cycles (100 kyr eccentricity cycle, 41 kyr obliquity cycle and 23 kyr precession cycle), primarily modulate the orbital scale climatic changes (Berger and Loutre, 1991;

Ruddiman, 2001). The Indian monsoon, driven by the large-scale land-sea pressure gradient, is very sensitive to the earth's orbital parameters (Anderson and Prell, 1993). Several studies suggest an orbital scale variability in the Indian monsoon in the geologic past (Prell, 1984; Prell and Van Campo, 1986; Clemens et al., 1991; Imbrie et al., 1992; Colin et al., 1998; Saraswat et al., 2020). The 41 kyr obliquity cycle and 23 kyr precession cycle strongly controlled the summer monsoon variability in the last 350 kyr (Clemens et al., 1991; Colin et al., 1998). The modelling studies have also confirmed the orbital scale control of the Northern Hemisphere insolation on the summer monsoon variability (Kutzbach, 1981; Kutzbach and Guetter, 1986; Prell and Kutzbach, 1987; de Noblet et al., 1996; Bosmans et al., 2018; Tejavath et al., 2021).

The signatures of change in the orbital configuration are widely observed in various paleoclimate records, including the monsoon. However, interestingly, a major change in paleoclimatic records is observed during the Pleistocene, without any concomitant reorganization of the orbital configuration. This change during the Pleistocene, termed as the mid-Pleistocene Transition (MPT: 1250 ka – 700 ka), is one of the most significant events for paleoclimatologists regarding global climate change (Maslin et al., 1998). During the MPT, climate signatures shifted from the dominant 41 kyr glacial-interglacial cycle to the 100 kyr cycle (Clark et al., 2006). The implications of the MPT are also evident in the global sea level (Rohling et al., 2014), sea surface temperature (Herbert et al., 2010), ice volume (Lisiecki and Raymo, 2005) and monsoon (DeMenocal, 1995). A weaker Indian summer monsoon post MPT is inferred based on the changes in clay mineralogy (Chen et al., 2019; Lee et al., 2020). However, a momentous event such as this demands more studies using different proxies with better resolution.

Several attempts were made to reconstruct the past monsoon changes from the Bay of Bengal (e.g., Duplessy, 1982; Kudrass et al., 2001; Govil and Naidu, 2011; Nilsson-Kerr et al., 2019; Lauterbach et al., 2020; Suokhrie et al., 2018; 2022). But, only a few of them have investigated the monsoon variability on the orbital time scale (Lee et al., 2020; Mcgrath et al., 2021; Clemens et al., 2021). Additional long-term studies are required to understand the effect of MPT on the Indian monsoon.

The monsoon intensity modulates the ocean's primary productivity. The primary productivity is an important climate modulator as it controls the ocean-atmosphere CO<sub>2</sub> exchange (Broecker, 1982). The primary productivity depends on many factors, including nutrient availability, turbidity, and light and wind intensity. The monsoon strongly controls these parameters. Therefore, primary productivity signatures are often used to assess the changes in monsoon intensity. Thus, the

paleoproductivity records will help understand the past monsoon-induced changes in these parameters.

The past productivity changes have been constructed by using different proxies (Muller and Suess, 1979; Berger et al., 1989; Pattan et al., 2003) like planktic foraminifera (Prell and Curry, 1981; Singh et al., 2006; Naik et al., 2017), benthic foraminifera (Herguera and Berger, 1991; Singh and Gupta, 2005), biogenic opal (Lange, 1993) and carbonate content (Wefer et al., 1999). Planktic foraminifera have been extensively used for paleoclimatic studies due to their wider availability and sensitivity towards the environment (Saraswat, 2015; Hollstein et al., 2017). Because of their direct response to the oceanographic conditions, planktic foraminifera have been considered excellent paleomonsoon indicators (Cullen and Prell, 1984; Hemleben et al., 2012; Curry et al., 1992; Schiebel et al., 2004). The effect of the Indian summer monsoon (ISM) on surface water productivity in the Bay of Bengal is still ambiguous. Some studies have reported reduced productivity during the summer monsoon season due to strong stratification, increasing turbidity, and light limitation (Madhupratap et al., 2003). In contrast, others have reported high productivity due to increased nutrients from riverine flux, upwelling or eddy pumping (Prasanna Kumar et al., 2004).

In this paper, we reconstruct the changes in the relative strength of the Indian summer and winter monsoon during the last 1.45 myr and the role of MPT in this. The productivity changes in the western Bay of Bengal with respect to monsoon are also discussed. We use different assemblages of planktic foraminifera as a proxy for this study. We also explore the implications of orbital periodicities on the Indian monsoon.

## **2. Regional Setting**

The International Ocean Discovery Program (IODP) Site U1446, drilled during IODP Expedition 353, is located 75 km from the east coast of India, offshore the Mahanadi Basin in the western Bay of Bengal at a water depth of 1441 m (Figure 1). The strategic location at a northwest-southeast trending ridge on the lower slope makes the site safe from any turbidite deposits. Dark to light grey clays dominate the drilled sediments with varying proportions of foraminifera, biosilica and nannofossils (Clemens et al., 2016). The average lithogenic fraction is 70%.

The northwestern Bay of Bengal is an atypical, unique basin perfect for paleomonsoon studies owing to its prime location in the core monsoon region, with the high terrestrial influx

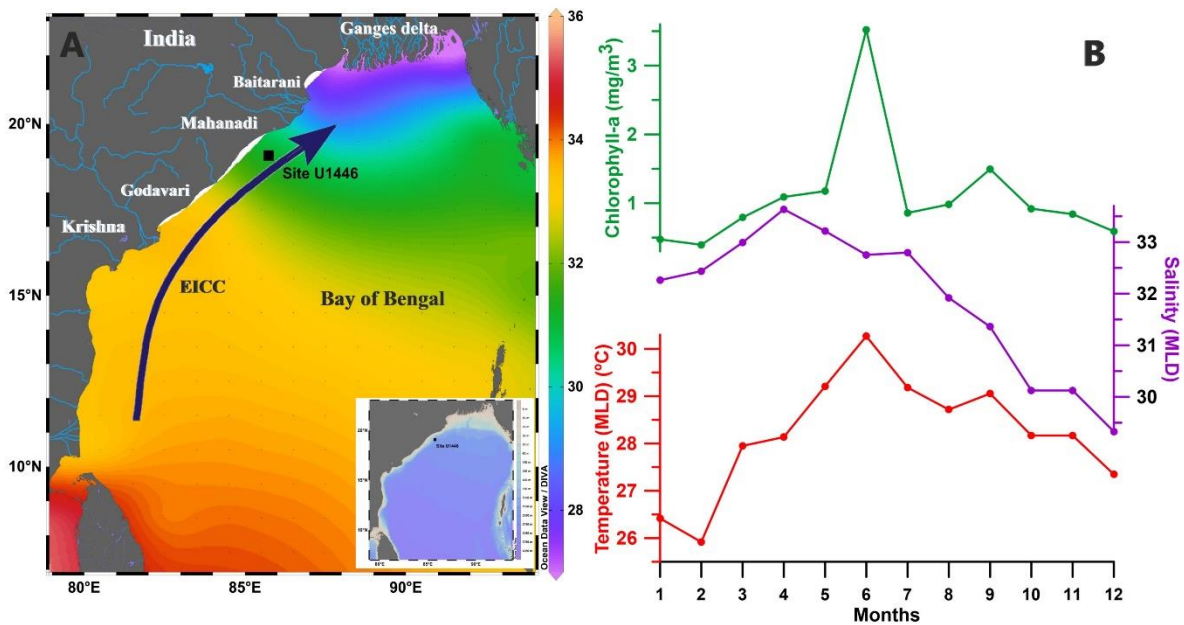


**Figure 1: (A) The location (black filled square) of Site U1446 in the core monsoon and riverine influx region of the western Bay of Bengal. The background contour is sea surface salinity during the summer monsoon season (July-September). The direction of the East Indian Coastal Current (EICC) during the summer monsoon season has been obtained from Schott et al. (2009). (B) The surface chlorophyll-a concentration and the Mixed Layer Depth (MLD) (0-25 m) temperature (°C) and salinity during different months at the site are also plotted. Source: World Ocean Atlas 2018 and SeaWiFS, accessed by Live Access Server, CSIR-NIO (Locarnini et al., 2018; Zweng et al., 2019).**

and high sedimentation rate. There is a net positive water flux of  $152 \times 10^{10} \text{ m}^3/\text{y}$  in the Bay of Bengal caused by the direct rainfall and riverine influx (Varkey et al., 1996). The net freshwater inflow to the Bay of Bengal peaks in June-October (Sengupta et al., 2006; Papa et al., 2012). The high riverine influx and a narrow continental shelf help in a huge influx of terrestrial matter up to the slope and further deeper regions. The higher food availability due to the riverine nutrient flux can increase the foraminiferal productivity in the region. However, the ensuing low salinity could be detrimental to some high salinity preferring species like *Globigerinoides ruber* (Bhadra and Saraswat, 2021). The surface salinity stays low, creating a shallow halocline at 5-20 m depth during the summer, autumn and winter (Thadathil et al., 2002; Helber et al., 2012). The springtime (March-May) salinity is typically high. The summer monsoon winds induce upwelling in the marginal regions of the western Bay of Bengal (Shetye et al., 1991). The upwelling increases nitrate availability, thereby increasing the primary productivity (Muraleedharan et al., 2007), an important factor for the planktic foraminiferal abundance, especially for the species like *Globigerina bulloides*

(Prell and Curry, 1981; Gupta et al., 2003). A major fraction of the riverine influx flows along the coastal region as East India Coastal Current (EICC) (Shetye et al., 1996; Chaitanya et al., 2014). The EICC flows southward, carrying low saline water during the peak summer monsoon. Post summer monsoon, EICC changes direction and flows northward, transporting high saline water (Shetye, 1993). During the winter monsoon, the EICC again changes direction and flows southward (Varkey et al., 1996).

The monthly temperature and salinity of the mixed layer (0-25 m) and the surface chlorophyll-a content at the drill site from the year 1986 were plotted to understand the influence of monsoon on productivity (Figure 1). The temperature and salinity data were obtained from the World Ocean Atlas-2018 (Locarnini et al., 2018; Zweng et al., 2019), and the chlorophyll-a data was obtained from the SeaWiFS chlorophyll data by using the Live Access Server of CSIR-National Institute of Oceanography, Goa, India. The chlorophyll-a concentration is very high during June, the time for the beginning of summer monsoonal rainfall. The highest salinity is during April, and the lowest is during December. The temperature is low during the winter (December-February) and warms during the summer (May-July) (Figure 1).

### **3. Methodology**

A total of 328 samples covering the entire 202 m drilled depth of the primary splice of IODP Site U1446 have been used for this study (See Appendix). The samples were collected at an interval of ~60 cm, corresponding to an age interval of ~4 kyr. All the samples were processed following the standard procedure (Saalim et al., 2017). The samples were collected in small, labelled and pre-weighed glass petri-dishes and frozen (-30°C) for 24 hours. The frozen samples were freeze-dried using a lyophilizer. The dry sediment samples were weighed and then washed using a 63 µm mesh-sized sieve. The material retained on the sieve (>63 µm, was dried, weighed and transferred to storage vials. A representative split aliquot of the original dried >63 µm fraction was sieved with a 125 µm sieve. Both the representative split fraction taken for sieving and the one obtained after sieving at 125 µm were weighed. From one-quarter of the fraction >125 µm, a minimum of 300 planktic foraminifera were picked using a stereo zoom microscope (Olympus SZX16) and mounted on a micropaleontological slide. All intact planktic foraminifera were picked from such fractions. The entire >125 µm size fraction was used wherever 300 planktic foraminiferal shells were not available. The number of individuals of different planktic foraminifera species was counted. The species were identified following Parker (1962), Schiebel and Hemleben (2017) and other literature.

The chronology of the Site U1446 was developed by Clemens et al. (2021) by using the 53 age tie-points (Figure 2). Of the 53 tie-points, four were accelerator mass spectrometer (AMS) radiocarbon dates between 1.7 and 6.1 m, one from the base of Toba ash at 15.6 m and the rest (48) from the comparison of benthic foraminifera oxygen isotopic ratio ( $\delta^{18}\text{O}$ ) with the global  $\delta^{18}\text{O}$  stack (Lisiecki and Raymo, 2005). The samples cover a time span of 1.45 myr with an average sample resolution of  $\sim 4$  kyr. The sedimentation rate is very high during the late Quaternary (up to 80 cm/kyr). Prior to 250 ka, the sedimentation rate varies between 5 and 20 cm/kyr (Figure 2).

The species were grouped into summer and winter monsoon assemblages for a more robust reconstruction of the seasonal monsoon changes. Both the modern surface distribution of the planktic foraminifera in the western Bay of Bengal (Bhadra and Saraswat, 2021) as well as sediment trap results (Guptha et al., 1997; Stoll et al., 2007) were used to define the characteristic monsoon assemblages.

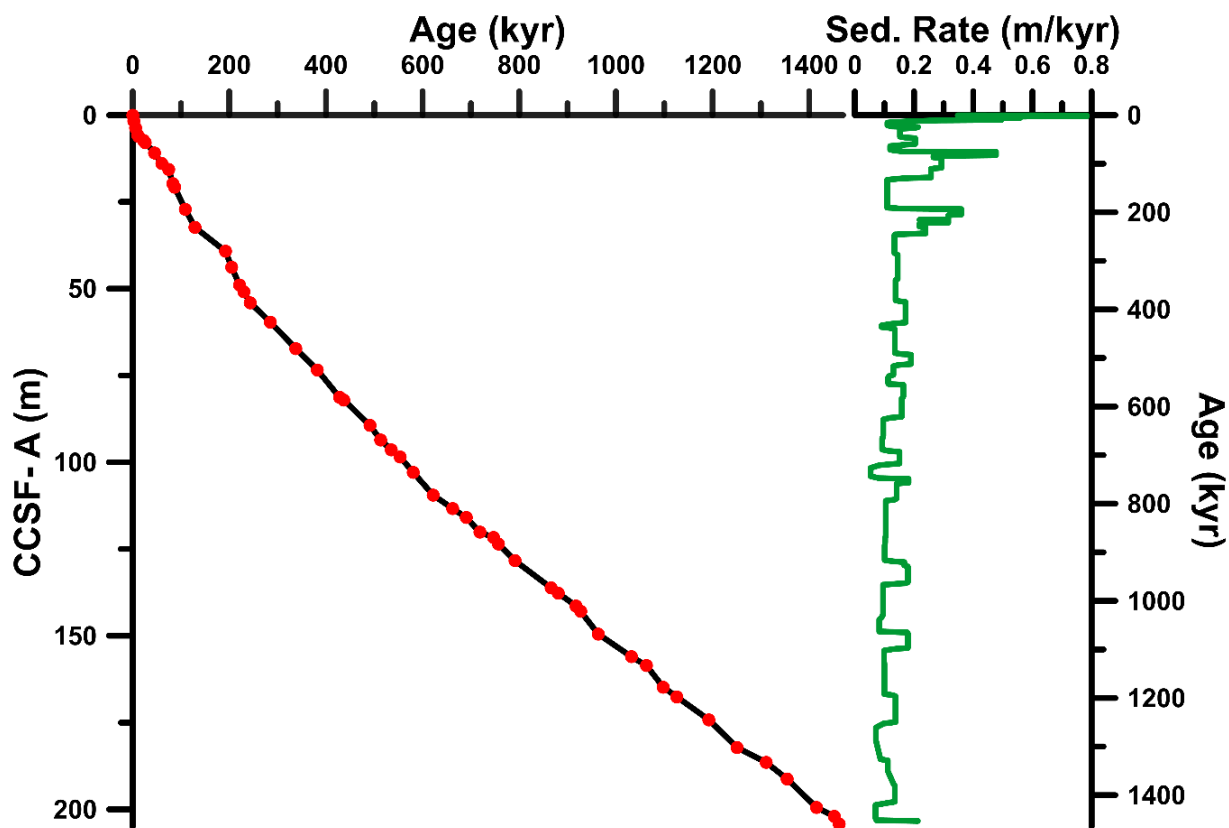


**Figure 2:** Left panel shows the composite core depth below sea floor (CCSF) against the age of Site U1446. The red-filled circles are the stable oxygen isotopic ratio ( $\delta^{18}\text{O}$ ) based tie points used to establish the chronology (Clemens et al., 2021). The right panel (thick green line) shows the temporal variation in the sedimentation rate (m/kyr).

*Globigerina bulloides*, *Globigerinella siphonifera*, *Trilobatus sacculifer* and *Neogloboquadrina dutertrei* were included in the summer monsoon assemblage (SMA) as their relative abundance increased during the summer monsoon months. *Globorotalia menardii* was included in the winter monsoon assemblage (WMA) as its relative abundance increased only in the winter monsoon season. Although *Globigerinita glutinata* was the most abundant species at Site U1446, it was excluded from the summer and winter monsoon assemblages because it was abundant during both seasons. *Globigerinoides ruber* abundance was also not restricted to any particular monsoon season in the Bay of Bengal (Guptha et al., 1997). However, this species has been extensively used as a winter monsoon indicator in the Arabian Sea (Caley et al., 2011; Saraswat et al., 2020). *Globigerina falconensis* is considered a typical winter monsoon species, and it represents a non-upwelling condition (Conan and Brummer, 2000; Peeters and Brummer, 2002; Schulz et al., 2002). The modelling studies suggest that the strong winter conditions shift the faunal assemblage from *G. bulloides* to a higher abundance of *G. falconensis* (Munz et al., 2015). The average and maximum relative abundance of *G. falconensis* at Site U1446 are 3.53% and 34.86%, respectively, which is quite significant. Therefore, *G. ruber* and *G. falconensis* have been included in the winter monsoon assemblage as well.

Different planktic foraminiferal species have been grouped into eutrophic and oligotrophic assemblages according to their ecological preference. *Globigerinita glutinata* is often associated with high phytoplankton productivity (Schiebel and Hemleben 2000; Chapman 2010). *Globigerina falconensis*, however, though it prefers eutrophic conditions, is less opportunistic in terms of food availability than *G. glutinata* and *G. bulloides*. The diet of *G. bulloides* and *N. dutertrei* consists of algae, whereas *T. sacculifer* uses copepods as its food (Schiebel and Hemleben, 2017). Therefore, *T. sacculifer*, *G. ruber* and *Globigerinoides conglobatus* are considered oligotrophic species because of their preference to warm low productive waters (Bé and Hutson, 1977; Stoll et al., 2007; Sears et al., 2012). So, these species have been included in the oligotrophic assemblage. *Globigerina bulloides*, *G. glutinata*, *G. falconensis* and *N. dutertrei*, though preferring different habitats, have one thing in common between them, namely preference for a high food availability environment. Because of their high organic matter preference, all these species have been traditionally termed as eutrophic species (Singh et al., 2018). Therefore, the combined relative abundance of all these species was used as a productivity indicator and termed as eutrophic assemblage.

In order to infer any cyclicity in the paleomonsoon and assess the effect of the long-term periodic global climatic changes on the Indian monsoon, wavelet and spectral analyses were done on the monsoon and productivity proxies by using the Past 4.03 software (Hammer et al., 2001). The



wavelet plots were generated through wavelet analysis for unequally spaced data. The spectral analysis was done using the REDFIT algorithm with a Rectangle window. The period between ~1250 ka and ~700 ka is generally considered as MPT (Maslin et al., 1998). As our dataset suggests a distinct change at MIS 22, we have taken 925 ka as a boundary to see the changes in cyclicity in the post MPT period. An oversample of 2 and a segment of 3 were taken as sub-parameters for the dataset between 925 ka and present. Due to fewer data points between 925 ka and 1450 ka, a segment of 2 was taken for spectral analysis.

#### **4. Results**

A total of 33 species belonging to 15 genera constitute the planktic foraminifera assemblage of the Site U1446. *Globigerinita glutinata* is the most abundant species. Other abundant species are *Globigerinoides ruber*, *Globigerina bulloides* and *Neogloboquadrina dutertrei* (Figure 3). The combined average relative abundance of these four species is ~75% at Site U1446. The average, maximum and minimum relative abundance of *G. glutinata* was 37.06%, 81.56% and 10.26%, respectively, indicating its dominant presence in the assemblage, irrespective of the environmental condition. The average abundance of *G. glutinata* increases from Marine Isotopic Stage (MIS) 45 to MIS 23 and decreases subsequently until the present (Figure 3). The average abundance of *G. ruber* is 17.13%, varying from a minimum of 4.05% to a maximum of 47.65%. Overall, the relative abundance of *G. ruber* shows a decreasing trend from 1.4 Ma to the present. Distinct short-term periodic peaks and lows are superimposed on the long-term decreasing abundance of *G. ruber*. The highest abundance of *G. ruber* is in MIS 12. A prominent low relative abundance of *G. ruber* is observed between ~650 ka and ~450 ka. *Globigerina bulloides* is abundant during most of the warmer interstadials and low during colder stadials.

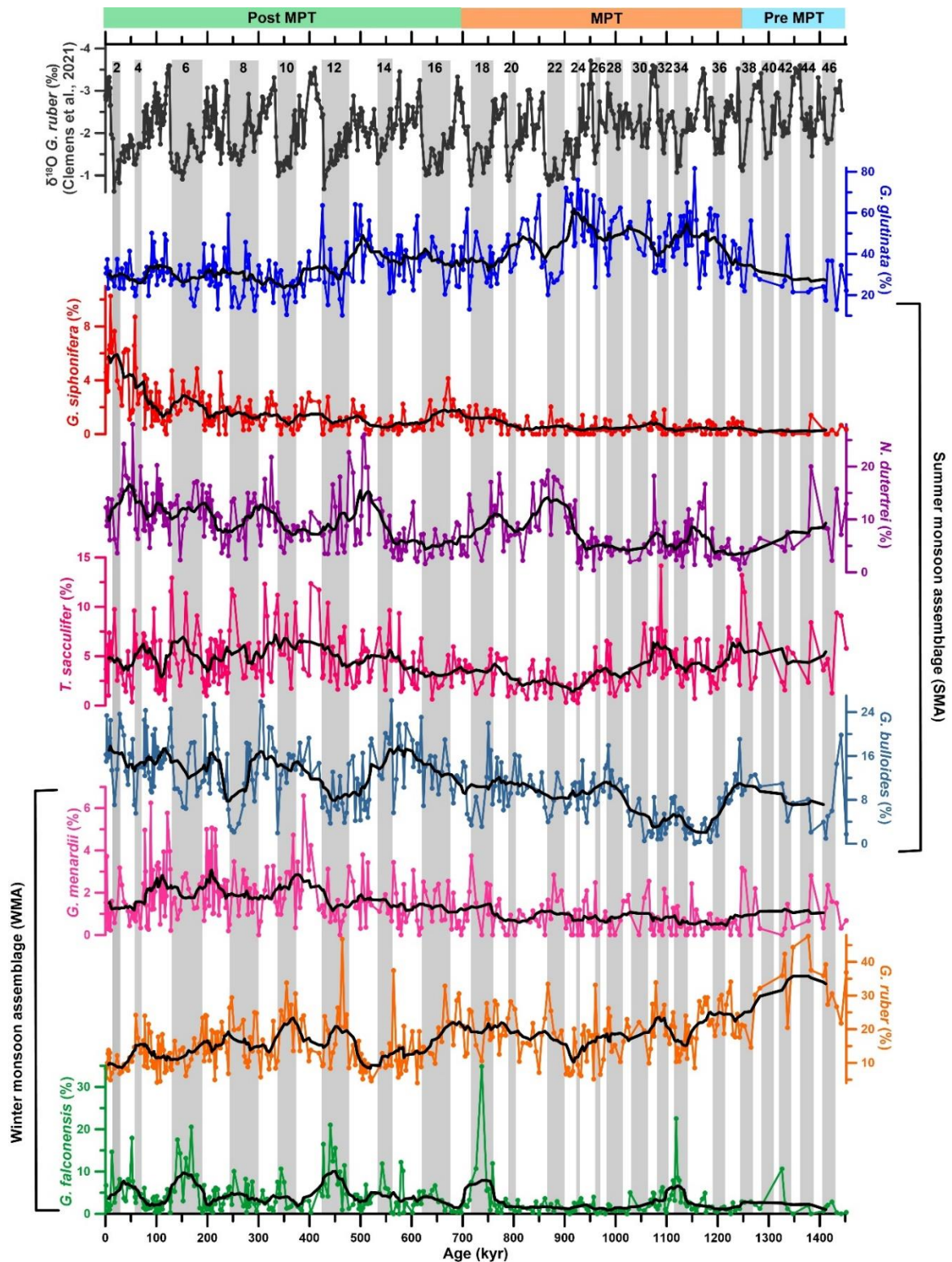


Figure 3: The relative abundance of all the major planktic foraminiferal species at Site U1446 along with the *G. ruber*  $\delta^{18}\text{O}$  obtained from Clemens et al. (2021) during the last 1.45 myr. The grey bars represent even-numbered MIS and have been marked by respective MIS numbers at the top. The intervals prior, during and post mid-Pleistocene Transition (MPT) have also been marked. Almost all the species show a large variation in the relative abundance during the stadial-interstadials. Additionally, several species (*G. siphonifera*, *G. glutinata*, *G. ruber*) also show a prominent linear increase or decrease throughout the last 1.45 myr. The running average (11 point) is plotted as thick black lines to better represent the long-term increasing or decreasing trend.

The average abundance of *G. bulloides* is 11.26%, with a minimum and maximum abundance of 0% and 26.14%, respectively. A prominent peak in the relative abundance of *G. bulloides* is observed between MIS 42 and MIS 36. The relative abundance was low during the early MPT (MIS 36 - MIS 30). However, the relative abundance of *G. glutinata* was high during this interval.

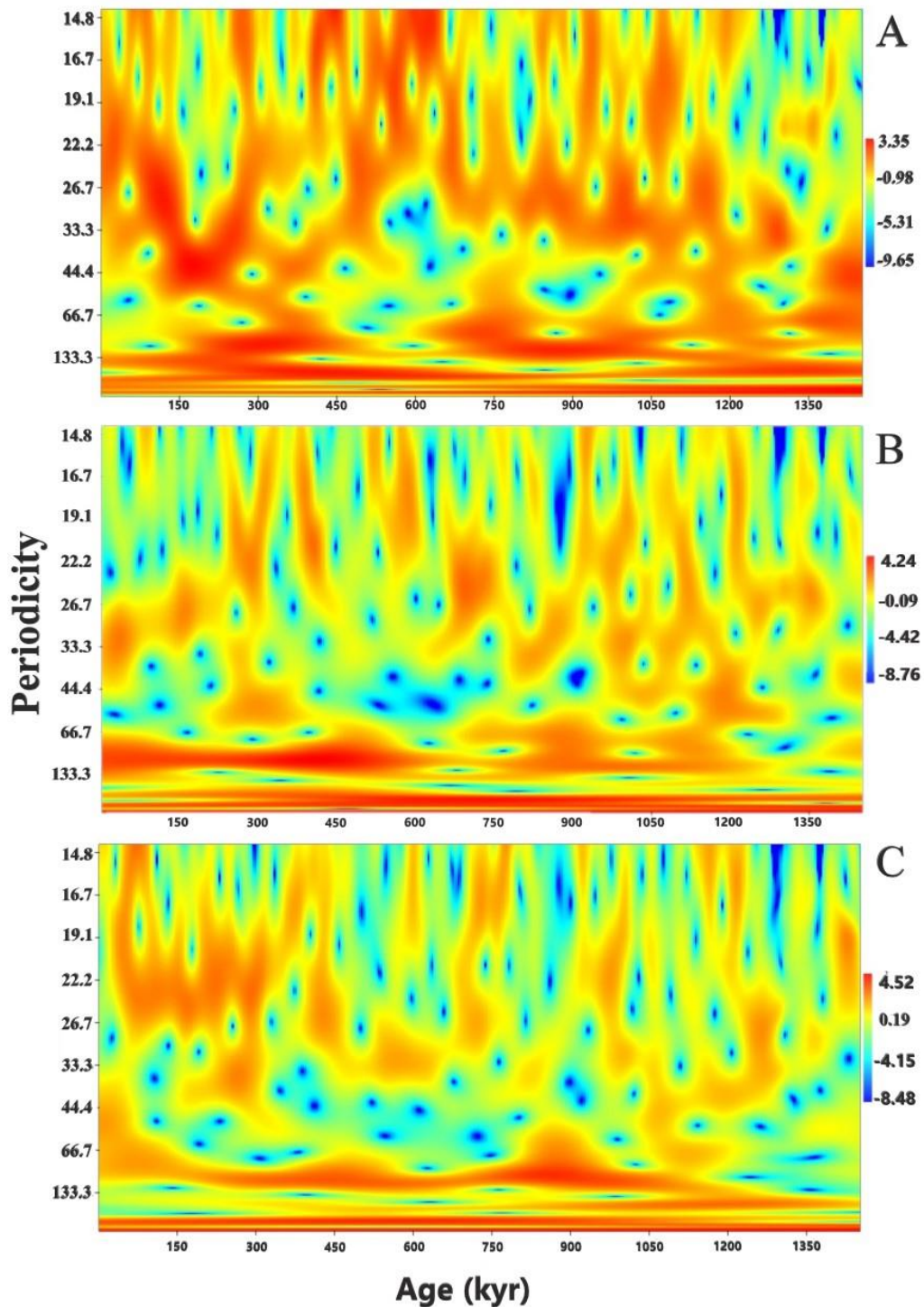
The stadial-interstadial variability in the relative abundance of *G. bulloides* increased significantly during the last ~350 kyr. Most of the peaks in the relative abundance of *N. dutertrei* are during warmer intervals, although this relationship is not consistent throughout. *Neogloboquadrina dutertrei* has an average abundance of 8.84%, varying from a minimum of 0.42% to a maximum of 27.98%. *Trilobatus sacculifer*, with an average relative abundance of 4.41%, is also more abundant during the interstadials. Its relative abundance is low during the MPT and high during both pre and post-MPT times. The minimum and maximum relative abundances of *T. sacculifer* are 0.26% and 14.16%, respectively. Interestingly, the relative abundance of *T. sacculifer* was very low throughout the MPT, as compared to the interval prior to and post-MPT. *Globorotalia menardii* does not follow any consistent trend during the stadial-interstadial. However, after ~350 ka, the stadial-interstadial variation in its relative abundance is similar to that in *G. bulloides*. The average relative abundance of *G. menardii* is 1.44% varying from being absent to the maximum of 6.59% but increases after MIS 12. *Globigerina falconensis* is comparatively more abundant in almost all cold stadials. *Globigerina falconensis* shows the most significant stadial-interstadial transition in its relative abundance among all the species. However, its relative abundance was <5% during the larger part of the last 1.45 myr. Its average relative abundance was 3.53%, varying from being completely absent to 34.86%. The average relative abundance of *Globigerinella siphonifera* is 1.32%, showing a constant linear increase from 1.45 Ma to the present. Its minimum and maximum relative abundances are zero and 10.27%, respectively (Figure 3).

The wavelet analysis for SMA shows significant 100 kyr variability during 1050 -700 ka and 500-150 ka. The 41 kyr cyclicity is present during 300-100 ka, and the 23 kyr cyclicity is present primarily throughout after 1200 ka. In the wavelet plot of WMA, the 100 kyr cyclicity is present in the entire studied interval, more significantly after 600 ka. The 41 kyr cyclicity is almost absent in the WMA wavelet plot. The eutrophic assemblage wavelet plot shows a cyclicity close to 100 kyr in the entire period after 1200 ka and the 23 kyr signal after 350 ka (Figure 4).

In the spectral analysis using REDFIT algorithm, the summer monsoon assemblage shows 22 kyr and 115 kyr periodicities after 925 ka with 95% and 90% significance, respectively. It shows a 100 kyr periodicity with 90% significance, between 925-1450 ka. The winter monsoon assemblage shows 102 kyr and 20 kyr periodicities with 99% and 95% significance after 925 ka, respectively.

Prior to 925 ka, it shows 26 kyr and 100 kyr periodicities with 95% and 90% significance, respectively (Figure 5). The eutrophic assemblage shows 102 kyr and 23 kyr periodicity after 925 ka with a significance of 99% (Figure 5). It shows 100 kyr and 23 kyr periodicities with 95% and 90% significance, respectively, between 925-1450 ka.

**Figure 4: The wavelet analysis of (A) summer and (B) winter monsoon assemblages. The periodicity in the eutrophic assemblage (C) was also plotted. The y-axis is periodicity, and the x-axis is age (kyr).**





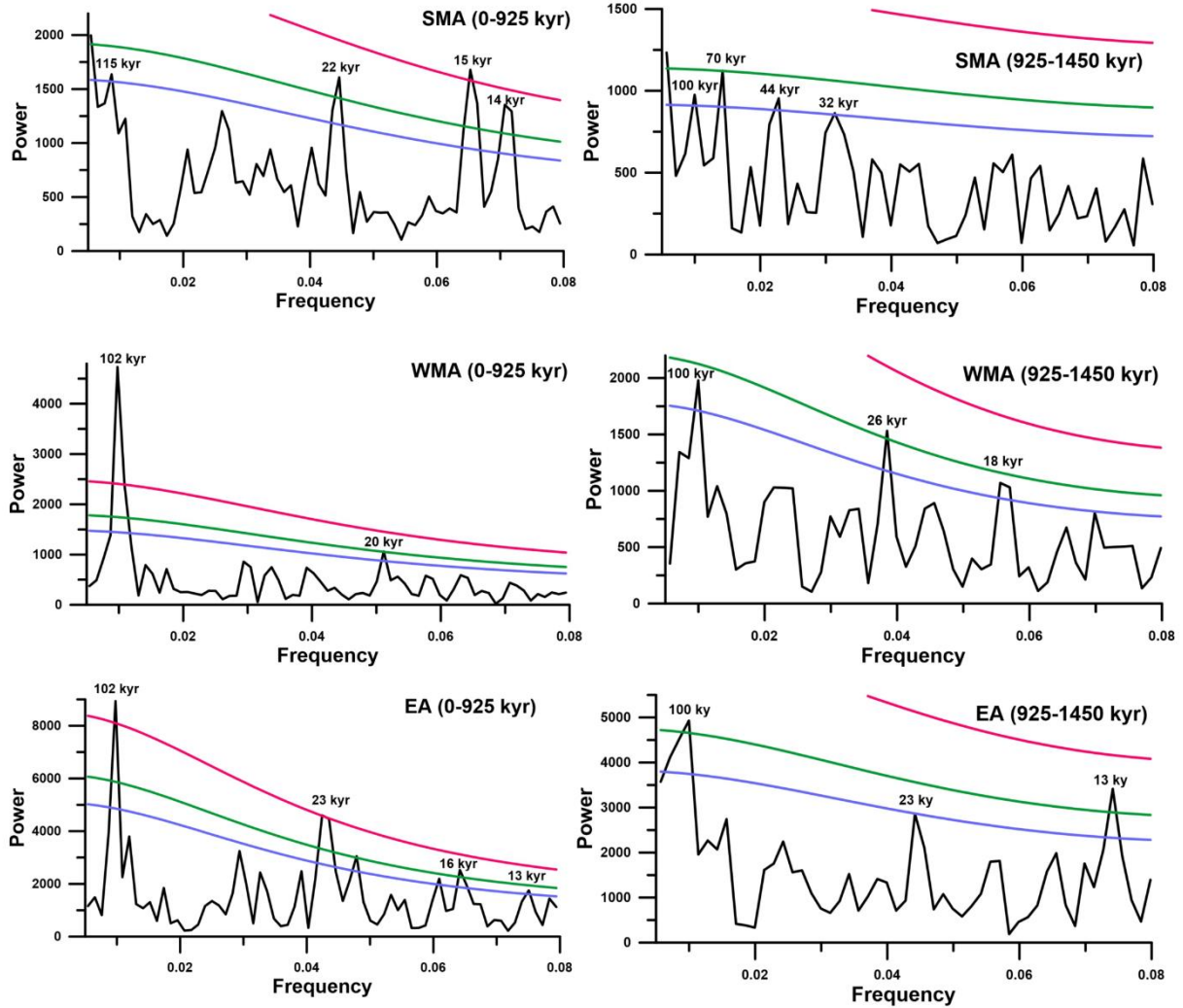


**Figure 5: The spectral analysis of summer and winter monsoon assemblage and eutrophic assemblage in the pre and post-MPT period (925-1450 ka and 0-925 ka, respectively). The blue, green and pink lines represent 90%, 95% and 99% significance, respectively. The significant periodicities are marked with the respective age. The y-axis is power, and the x-axis is frequency.**

## 5. Discussion

### 5.1 Ecological interpretation of the planktic foraminiferal assemblages

Although *G. glutinata* is the most abundant species throughout the studied interval, its relative abundance continuously decreases from MIS 22 until the present. At the same time, the relative abundance of other typical summer monsoon species like *G. bulloides*, *G. siphonifera*, *N. dutertrei* and *T. sacculifer* increased post-MPT period (Figure 3). In a recent surface distribution study of the planktic foraminiferal species, *G. glutinata* was found to be highly abundant in the Bay of Bengal and was related to the high nutrient availability from the riverine influx as well as better preservation of its tests (Bhadra and Saraswat, 2021). *Globigerinita glutinata* is an opportunistic species and is

often related to colder conditions (Schiebel et al., 2001; Bhadra and Saraswat, 2021). Schiebel and Hemleben (2000) linked the high relative abundance of *G. glutinata* to the mixed layer deepening in the north Atlantic. However, it should be noted that *G. glutinata* in this study has been picked from >125 µm size fraction, which can render size-related bias when compared to the studies that used >150 µm fraction.

*Neogloboquadrina dutertrei* is essentially thermocline dwelling species (Thunell and Reynolds, 1984; Schiebel and Hemleben, 2017). Also, its abundance increases with increased stratification. Therefore, the relative abundance pattern of *N. dutertrei* indicates a warmer and more stratified Bay of Bengal post-MPT. The signal, however, is continuous from MIS 22 until the present, suggesting a strengthening of the summer monsoon. *Globigerinoides ruber* and *T. sacculifer* are considered oligotrophic species because of their preference to warm low productive waters. The only difference is that *G. ruber* prefers high saline waters (>36) (Bhadra and Saraswat, 2021), whereas *T. sacculifer* is mainly found in comparatively less saline waters (<36) (Bé & Hutson, 1977; Sears et al., 2012). This would explain the different trends in the relative abundance of both these species post-MPT. The lower surface salinity in the western Bay of Bengal because of high riverine influx and precipitation due to a strengthened monsoon was detrimental to *G. ruber*.

*Globigerina bulloides* is fairly abundant at Site U1446. Its relative abundance reaches more than 20% in the post-MPT interstadial periods (Figure 3). *Globigerina bulloides* has been used as a robust summer monsoon intensity proxy in the Arabian Sea (Overpeck et al., 1996; Gupta et al., 2003; Naik et al., 2017). It prefers relatively cold, nutrient-rich high productive water (Curry et al., 1992; Schiebel et al., 2001) and has been suggested as an upwelling indicator species in the lower latitudes (Anderson and Prell, 1993; Conan and Brummer, 2000; Gupta et al., 2003; Sears et al., 2012). The high abundance of *G. bulloides* during interstadials indicates stronger upwelling in the northwestern Bay of Bengal. *Globigerina bulloides* (%) shows a good match with  $\delta^{18}\text{O}$  of *G. ruber* on the glacial-interglacial time scale, more prominently MIS 22 onwards. However, the extent of variation in both does not show any overall similarity. This means that though there is upwelling during interstadials, the strength of upwelling is independent of the strength of the interstadial. The high abundance of *G. bulloides* during interstadials is similar to that in the Arabian Sea (Gupta et al., 2003), a highly productive basin with a robust summer upwelling.

## **5.2. Changes in the strength of the Indian monsoon in the last 1.45 myr**

The relative abundance of summer monsoon assemblage was higher in the warmer interstadial stages (e.g. MIS 3a, 5e, 9e, 13a, 19a, 31, 47) and lower during the colder stadial stages (e.g. MIS 2, 6c, 18e,

25d, 46) in most of the intervals, throughout the record (Figure 6). The winter monsoon assemblage shows the opposite trend, increasing during the stadials (e.g. MIS 8a, 12c, 18e, 22, 26, 44) and decreasing during the interstadials (e.g. MIS 1, 9c, 15e, 27, 47) (Figure 6). However, this trend is less significant before MIS 22, whereas it is more prominent during the post-MPT period, suggesting a stronger covariance of the Indian monsoon system with the glacial-interglacial variability post-MPT. In the western Bay of Bengal, the monsoon winds blow from the south to the north and induce upwelling along the eastern margin of India. The relative abundance of *G. bulloides* also peaks during the interstadial periods. Therefore, it is evident that the summer monsoon was strong during the interstadials and weak during the stadials throughout the last 1.45 myr in the western Bay of Bengal. A stronger summer monsoon during interstadials has been reported by several workers based on long-term records from the Indian Ocean (Kunkelova et al., 2018; Saraswat et al., 2019; Alvarez Zarikian et al., 2022). The scenario is exactly the opposite when it comes to the winter monsoon. The winter monsoon was stronger during the stadials as compared to the interstadials.

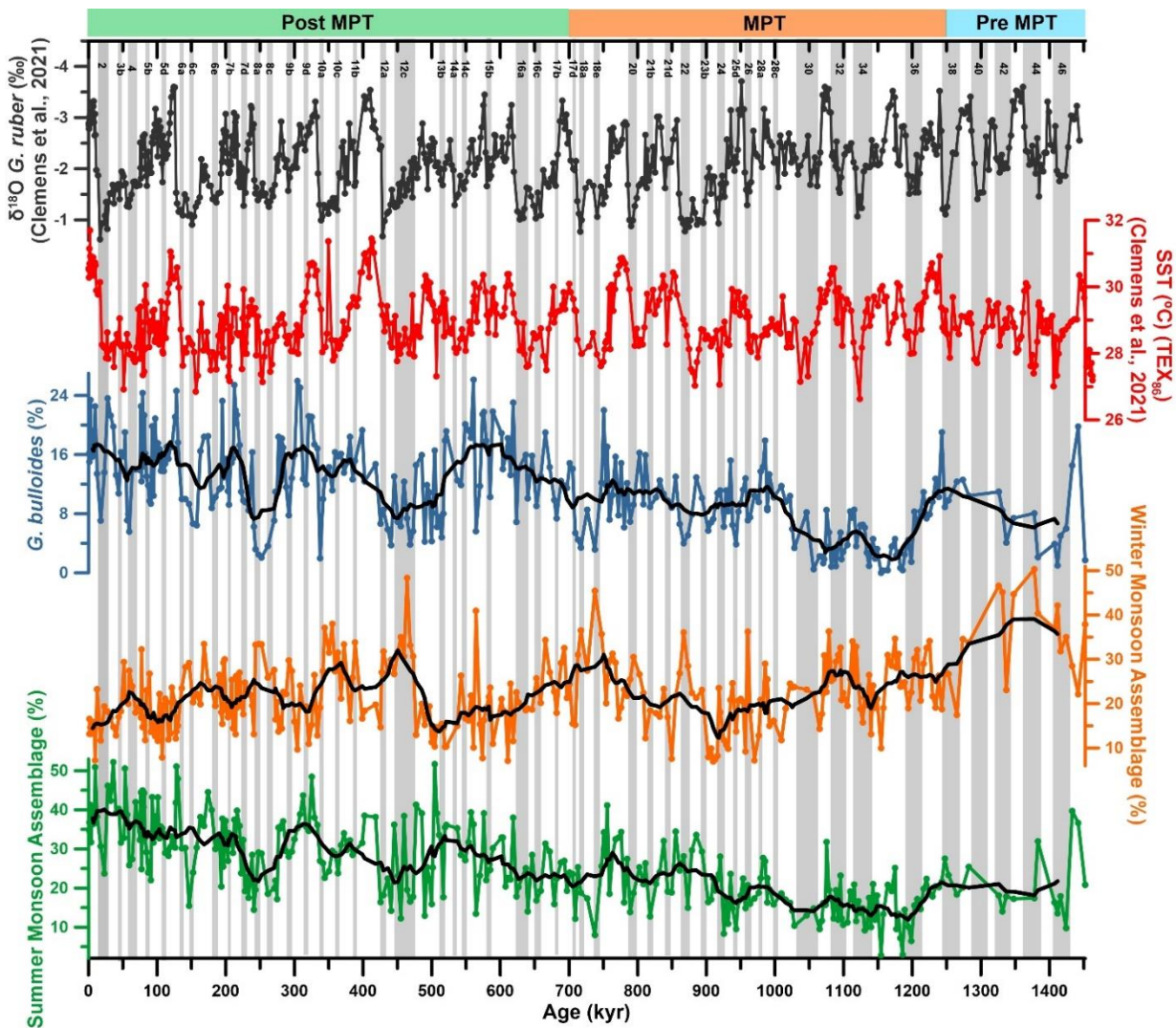


**Figure 6:** The summer and winter monsoon assemblages, as well as the relative abundance of upwelling indicator *G. bulloides*, are plotted with the tetra ether index (TEX<sub>86</sub>) sea surface temperature and *G. ruber*  $\delta^{18}\text{O}$  record of Site U1446 obtained from Clemens et al. (2021). The grey bands indicate stadal substages marked by the respective MIS number at the top. The sub-stage notations have been taken from Railsback *et al.* (2015). The intervals prior, during and post mid-Pleistocene Transition (MPT) have also been marked. A prominent stadal-interstadial variation is evident in both the summer and winter monsoon assemblages. Additionally, gradual strengthening of the summer monsoon is also observed post-MPT. The running average (11 point) is plotted as thick black lines to better represent the long-term increasing or decreasing trend.

Clemens and Prell (2003) prepared a summer monsoon stack for the last 350 kyr by combining five different summer monsoon proxies (grain size, barium mass accumulation rate, *Globigerina bulloides* (%), opal mass accumulation rate and nitrogen isotopic ratio) from the northwestern Arabian Sea, by using stacking and principal component analysis. They show an increase in summer monsoon strength during the interstadials. We compared the SMA with the summer monsoon stack of Clemens and Prell (2003). The summer monsoon assemblage of U1446 for the last 350 kyr very well matches the stack reconstructed by Clemens and Prell (2003) (Figure



7). The studies from the Arabian Sea have also reported stronger summer monsoon during the interstadials (Clemens et al., 1991; Zahn and Pedersen, 1991; Anderson and Prell, 1992; Emeis et al., 1995; Ivanova et al., 2003; Saraswat et al., 2020).

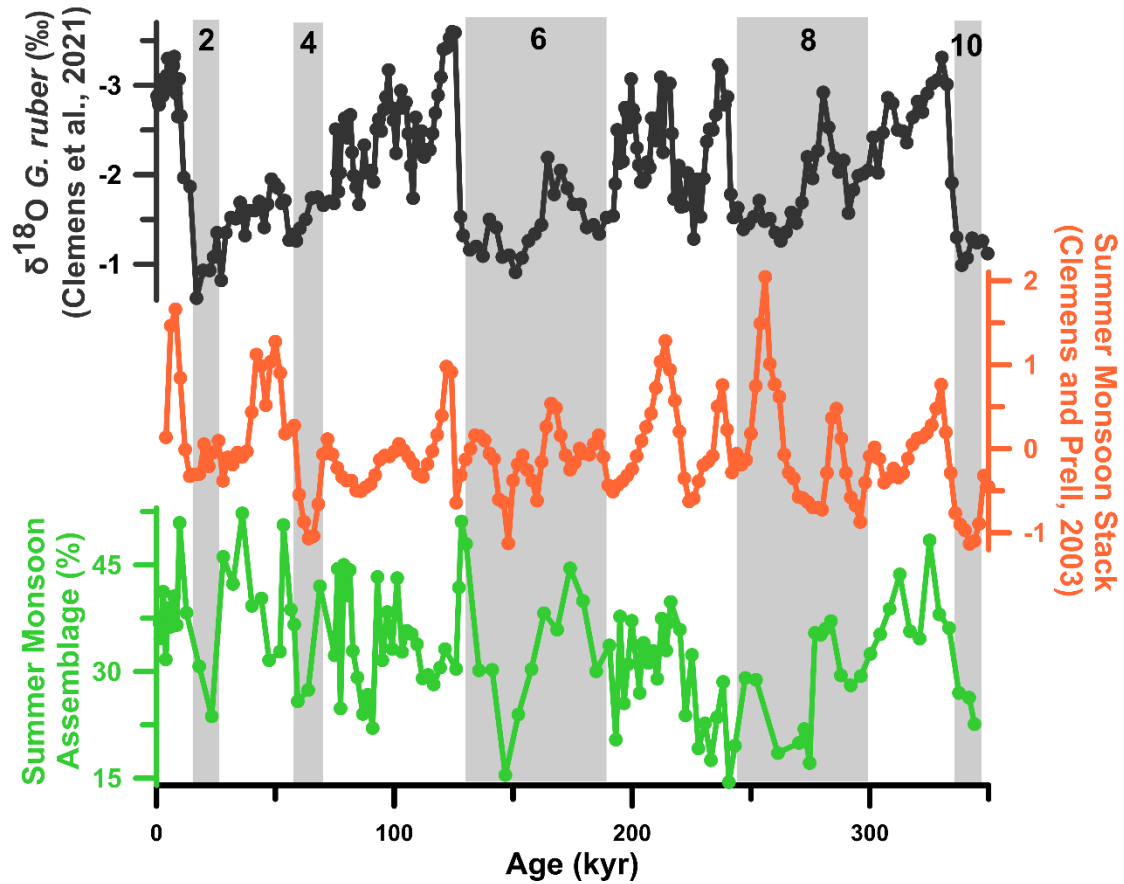


**Figure 7:** A comparison of the Site U1446 summer monsoon assemblage with the summer monsoon stack from the Arabian Sea prepared by Clemens and Prell (2003). The *G. ruber*  $\delta^{18}\text{O}$  at Site U1446 obtained from Clemens et al. (2021) is plotted for reference. The stadial-interstadial variations in the Site U1446 summer monsoon assemblage match well with the Arabian Sea summer monsoon stack. The grey bars represent even-numbered MIS and have been marked by respective MIS numbers at the top.

Lee et al. (2020) reported a decrease in summer monsoon intensity from 1.5 Ma to the present. They have reported high carbonate percentage and high relative abundance of *G. bulloides* in the post-MPT period and related it to the increased convective mixing due to the strengthening of the winter monsoon. They used the *G. bulloides* data of Mohan and Gupta (2011) from the southeast Arabian Sea. A strong winter monsoon wind condition would increase the convective mixing in the Bay of Bengal, which in turn enhances the nutrient availability in the surface mixed layer and increases the productivity. However, from the sediment trap studies (Guptha et al. 1997), it is clear that *G. bulloides* is much more abundant during the summer monsoon season than in the winter. We

also see an increase in the *G. bulloides* (%) after the MPT. In the U1446 record, the summer monsoon assemblage increases and the winter monsoon assemblage decreases during the post-MPT period (Figure 6). Thus, the high carbonate percentage reported by Lee et al. (2020) during the post-MPT period is because of increased upwelling induced by the strengthened summer monsoon and not due to the convective mixing caused by the enhanced winter monsoon.

Between MIS 32 and MIS 29, the *G. bulloides* abundance was low and increased afterwards until the present (Figure 6). There has been a continuous increase in the relative abundance of *G. bulloides* from the middle Pleistocene to the present. A similar but more prominent trend is seen in the summer monsoon assemblage (Figure 6). From this trend, it is clear that the summer monsoon was weak during MIS 34-36 and has continuously strengthened since then. However, the winter monsoon assemblage does not show any similar linear trend in the earlier part of the studied interval. The winter monsoon assemblage shows a more cyclic trend, and its percentage decreases steadily only after MIS 12. Overall, the average relative abundance of summer and winter monsoon assemblages are 25.8% and 22.1%, respectively, showing the almost equal impact of both the monsoons in the western Bay of Bengal, with summer monsoon being marginally dominant. However, a large change in the relative abundances of both summer and winter monsoon is observed during the post-MPT period (after 700 ka) with average values of 30.8% and 20.6%, respectively. The higher relative abundance of the summer monsoon assemblage suggests that the summer monsoon was dominant during the last ~650 kyr. Further, it is inferred that the winter monsoon weakened post-MPT as the summer monsoon strengthened. The studies on Chinese and Japanese loess deposits suggest the strengthening of the East Asian Summer Monsoon in two stages after 1.2/1.1 Ma and 550 ka, in line with the uplift of the Tibetan plateau (An et al., 1990; Xiao and An, 1999). We also report that on a longer time scale, the strength of the winter monsoon is not linearly correlated with the strength of the summer monsoon, which is in line with the findings from the equatorial Indian Ocean (Alonso-Garcia et al., 2019).

We suggest that the Indian summer monsoon was very weak during the early MPT period. It only started strengthening from MIS 22 (Figure 6). The period between MIS 35-31 was a warm period (McClymont et al., 2013; Teitler et al., 2015; Detlef et al., 2018). The global climate was arid between 1.2-1.0 Ma, as reported by several studies from different locations throughout the globe (Tiedemann et al., 1994; Clemens et al., 1996; Martínez-García et al., 2011). Jiang et al. (2019) related this to a combined effect of low eccentricity and low obliquity, which results in smaller contrast between summer and winter in the Northern Hemisphere and ice sheet expansion (Zachos et al., 2001). During MIS 24-22, the temperature dropped globally (Raymo et al., 2006; Prokopenko et

al., 2006; McClymont et al., 2013), and the Bering Sea was covered by ice (Kender et al., 2018). The Antarctic ice volume expanded (Elderfield et al., 2012), and the global thermohaline circulation weakened (Pena & Goldstein, 2014). The ISM intensified because of the increased cross-equatorial pressure gradient between the southern subtropical Indian Ocean and the Indian subcontinent due to the expansion of Antarctic ice sheets (Clemens et al., 1996; Elderfield et al., 2012; Farmer et al., 2019; Chen et al., 2020). This is in line with the increase in moisture variability in the Tibetan Plateau (Koutsodendris et al., 2018) during MIS 24-22. The stronger ISM-induced rainfall on the Indian subcontinent resulted in a high riverine influx to the western Bay of Bengal, which increased the stratification and, thereby, the SST (Shenoi et al., 2002). This explains the increase in average SST during interstadials in the post-MPT period (Figure 6).

The winter monsoon also weakened from MIS 46 until MIS 23 (Figure 6). It also started strengthening at MIS 22 and increased in strength along with the summer monsoon until MIS 18. Only after MIS 17 did the winter monsoon and summer monsoon follow more prominent opposite variability. Previously, an increase in the contrast between summer and winter monsoon is reported after the onset of MPT, resulting in colder winters and warmer summers (Clemens et al., 1996; Guo et al., 2000; Jiang et al., 2019). However, in our record, this change comes much later at MIS 18, during late MPT. This could be the reason for the larger variability in the ISM strength during the glacial-interglacial cycle post-MPT.

In the U1446 record, there are five intervals where the summer monsoon assemblage is >50% of the total abundance. While four of these intervals are within the last 130 kyr, only one interval is prior to that at ~504 ka in the MIS 13. The MIS 14-13 transition is the least prominent glacial-interglacial transition in terms of ice volume change post-MPT (Lisiecki and Raymo, 2005). There are several reports of cooler Antarctic temperature (Jouzel et al., 2007) and lower CO<sub>2</sub> and CH<sub>4</sub> concentrations (Louergue et al., 2008; Luthi et al., 2008) during the MIS 13, as compared to other interglacials. Some studies have argued in favour of a moderate variability in the strength of the Indian monsoon system during the MIS 13-14 because of smaller displacement of the ITCZ due to a reduced interhemispheric heat transport (Alonso-Garcia et al., 2019). We report a high variability in the summer and winter monsoon across MIS 13-14 despite a low variability in the ice volume change visible in the  $\delta^{18}\text{O}$  *G. ruber* record. The winter monsoon strengthened at the onset of MIS 14 to weaken again afterwards, whereas the summer monsoon reached its peak during the initiation of MIS 13a. In fact, these peaks are two of the most prominent ones in the entire record. The global methane concentration also increased during the MIS 13a (Spahni et al., 2005), indicating an expansion of global wetlands (Chappellaz et al., 1993). A few workers have also reported an anomalously high

East Asian summer monsoon intensity during MIS 13, which otherwise is considered a colder time (Guo et al., 2000; Sun et al., 2006; Yin and Guo, 2008; Guo et al., 2009; Hao et al., 2015). Oliveira et al. (2020) also reported increased land biomass in southwestern Europe during this period. We see a spike in the productivity record of Site U1446 as well during this interstadial (Figure 6). A similar increase in the productivity in the Arabian Sea during the MIS 13 was earlier attributed to the increased nutrient availability due to intensified overturning circulation at the end of the MPT (Ziegler et al., 2010). Any link between this high productivity event and strengthened summer monsoon intensity was ruled out. Subsequently, no specific reason was provided for this high productivity event (Caley et al., 2011). Recently, similar high productivity during interstadials in general, and MIS 13 in particular, has also been reported in the equatorial Indian Ocean, based on the increased abundance of alkenones at Site U1467 (Alonso-Garcia et al., 2019; Alvarez Zarikian et al., 2022). However, the light oxygen isotope event reported in the equatorial Indian Ocean (Bassnot et al., 1994) was attributed to a strengthened summer monsoon caused by a cumulative impact of obliquity and precession forcing. At Site U1446, however, this change (both in EA and SMA) is very prominent and atypical. Therefore, this high productivity event is attributed to an anomalous intensification of the summer monsoon.

MIS 12 presents the highest peak in the WMA during the last 1.45 myr in our record. The Termination V at the MIS 12-11 transition shows the highest amplitude shift in the  $\delta^{18}\text{O}$  *G. ruber* record (Figure 6) (Clemens et al., 2021). MIS 12 is considered one of the most severe glacial phases of the Quaternary, with the global ice volume being 15% more than that of the last glacial maximum, which resulted in the sea level being 140 m lower than present (Lisiecki and Raymo, 2005; Masson-Delmotte et al., 2010; Rohling et al., 2014). It was also a very dry period in the Indian Peninsula (Alonso-Garcia et al., 2019). In contrast, during MIS 11, the sea level rose to 20 m above than present time (Hearty et al., 1999; Rohling et al., 2014). The WMA decreased, and the SMA increased at MIS 11e, indicating a shift toward a strengthened summer monsoon and a weakened winter monsoon (Figure 6). In fact, the winter monsoon gradually weakened MIS 12 onwards until the present, making it a major turning point.

Gupta et al. (2010) related the abrupt decrease in *G. bulloides* (%) in the equatorial Indian Ocean from MIS 8 onwards to a shift towards a weak Indian Ocean Equatorial Westerly wind and positive Indian Ocean Dipole (IOD). A positive IOD has been reported to strengthen the Indian summer monsoon strength. During positive IOD, the western Indian Ocean becomes warmer (Hastenrath et al., 1993; Saji et al., 1999). The ISM has been suggested to increase in strength post-Mid Brunhes Event (MBE) (~430 ka) due to the weakening of Indian Ocean Equatorial Westerly

wind and strengthening of positive IOD. However, in our long-term record, we can see that the ISM started strengthening much before that and post-MBE strengthening is just a manifestation of the same (Figure 6). Alonso-Garcia et al. (2019) reported an increase in C<sub>3</sub> vegetation from MIS 13 to MIS 7 in the Indian Peninsula during the interstadial times, indicating a humid period which also corroborates our record.

Several studies have argued for a strengthened winter monsoon and weakened summer monsoon after the onset of the 100 kyr cycle owing to the southward shift of ITCZ due to the large ice cover on the Himalayas (Overpeck et al., 1996; Guo et al., 2012). Kunkelova et al. (2018) also suggested a strengthened winter monsoon at MBE. However, the U1446 record shows a weakened winter monsoon at MBE. Although the winter monsoon was strong during the stadials that followed the MBE, as compared to the interstadials, it saw an overall decline in strength in the last 480 kyr (Figure 6).

During MIS 1-2 transition, there is a huge shift in all the parameters (Figure 6). The sea surface salinity decreased, SST increased (Clemens et al., 2021), productivity increased, the summer monsoon strengthened, and the winter monsoon weakened. Our record corroborates several studies from the Bay of Bengal (e.g., Ahmad et al., 2008; Govil and Naidu, 2011; Tripathy et al., 2014; Lauterbach et al., 2020). The summer monsoon in the early Holocene was one of the strongest during the entire studied period.

### **5.3. Productivity changes in the western Bay of Bengal during the last 1.45 myr**

The eutrophic assemblage shows high abundance during the interstadials (eg. MIS 3, 5e, 11, 21, 35) and low abundance during the stadials (eg. 2, 4, 6, 8, 10, 12, 14, 22, 26, 30, 38, 46) (Figure 8). The oligotrophic assemblage (%) was high during colder MIS (eg. 4, 8, 10, 12, 14, 16, 22, 26, 28, 32, 44) and comparatively low during the warmer MIS (eg. 3, 5, 7, 9, 13, 15, 21, 23, 25, 35) (Figure 8).

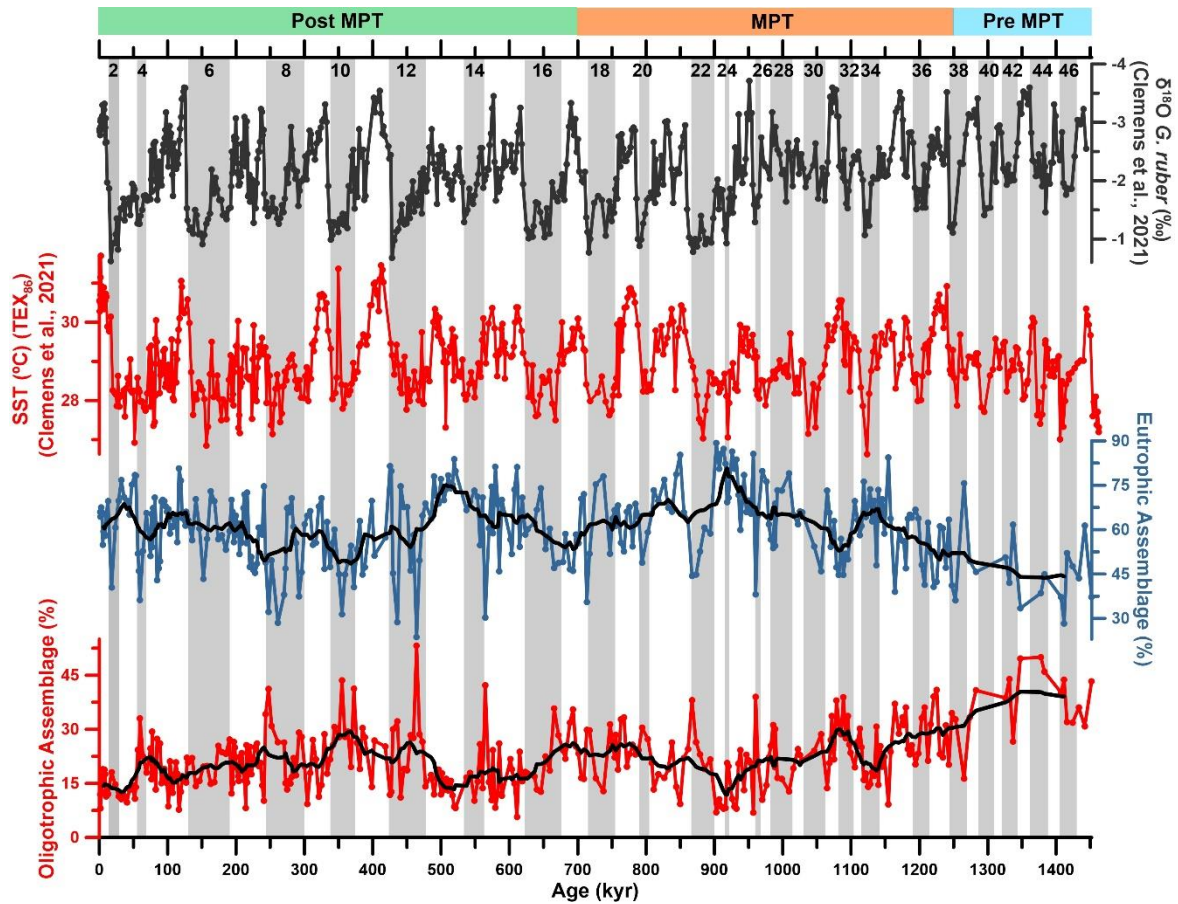


**Figure 8:** The eutrophic assemblage and the oligotrophic assemblage at Site U1446 during the last 1.45 myr is plotted with the *G. ruber*  $\delta^{18}\text{O}$  and SST record obtained from Clemens et al. (2021). The grey bands are even-numbered MIS marked by respective numbers at the top. The running average (11 point) is plotted as thick black lines to better represent the long-term increasing or decreasing trends.

During the interglacials, the strengthened summer monsoon must have caused intense upwelling and increased productivity in the western Bay of Bengal, creating a suitable environment for eutrophic species. The phytoplankton abundance in the Bay of Bengal is mainly controlled by the availability of nutrients (silicate, nitrate and phosphate) (Paul et al., 2008). The summer monsoon induced riverine influx brings a large amount of nutrients, mostly silicate, to the Bay of Bengal (Prasanna Kumar et al., 2002; Miranda et al., 2020). The summer monsoon induced upwelling at the same time also brings nutrients, mainly nitrate, to the surface (Sarma et al., 2016). The increase in overall nutrient availability in the surface mixed layer during the summer monsoon, therefore, increased the productivity in the western Bay of Bengal. Interestingly, the eutrophic assemblage also shows a good match with the SST variation (Figure 8). As all the species used in the oligotrophic assemblage prefer warm temperatures, it is expected that their abundance should increase with the increase in temperature. However, this is not the case here. Although the SST signal here is derived from  $\text{TEX}_{86}$ , which records the temperature of the near-surface to shallow subsurface (0-200 m)

(Zhang and Liu, 2018), it should be noted that the freshwater induced stratification in the western Bay of Bengal will warm the subsurface waters as well. This supports our earlier observation of high productivity during strengthened summer monsoon conditions and suggests that nutrient availability has greater control over the planktic foraminiferal species abundance than temperature.

During the winter monsoon, the strong temperature inversion in the northwestern Bay of Bengal creates a thick barrier layer (~50 m), which inhibits convective mixing, thereby decreasing nutrient availability in the surface waters. Furthermore, the thin barrier layer, along with the low latent heat flux, does not allow the cool water to come to the surface, causing a shallow mixed layer and warmer surface temperature compared to the Arabian Sea (Thadathil et al., 2002; Prasad, 2004; Balachandran et al., 2008). Thus, the bulk of the productivity in the western Bay of Bengal is controlled by the summer monsoon. Therefore, even though the winter monsoon was stronger during the stadials, productivity was lower than in the interstadials.

The oligotrophic assemblage decreased, and the eutrophic assemblage increased during the post-MPT period, especially after MIS 12 (Figure 8). This indicates an increase in productivity after the MPT in the western Bay of Bengal because of the strengthened summer monsoon, as discussed in the previous section. Additionally, a large seasonal change in salinity, as well as halocline and thermocline depths, will also strongly affect the productivity. A detailed reconstruction of the temporal changes in the upper water column stratification is required to understand its effect on productivity.

#### **5.4 Periodic changes during the last 1.45 myr**

From the spectral analysis, it is evident that there was absence of any precession control on the ISM prior to the MPT. However, the SMA is more affected by the 23 kyr precession cycle than the eccentricity cycle during the post-MPT period (Figure 5). Although the ISM is affected by both the eccentricity and precession cycle to some extent, other internal forcings like CO<sub>2</sub> concentration and ice volume changes also play a major role. Cai et al. (2015) reported dominance of 23 kyr precessional periodicity in the ISM. The speleothem studies show a predominant control of the summer insolation, i.e., changes in the external forcing on the ISM (Kathayat et al., 2016; Zhang et al., 2019), whereas McGrath et al. (2021) and Clemens et al. (2021) found the stronger ISM to be in phase with ice volume minima and CO<sub>2</sub> maxima. Colin et al. (1998) reported that the 23 kyr cycle is dominant during the last 280 kyr.

During the pre-MPT period, the WMA was controlled more by the precession forcing compared to the eccentricity forcing. The presence of a highly significant 100 kyr periodicity, the

low significance of the precession signal and the absence of the obliquity signal suggest that the Indian winter monsoon was greatly affected by the eccentricity cycle during the post-MPT period (Figure 5). The East Asian Winter Monsoon has also been reported to be strongly affected by the eccentricity cycle (Ding et al., 1995; Xiao et al., 1995). Yamamoto et al. (2013) suggested that the East Asian and Indian winter monsoon behaved synchronously in the East Asian and Indian regions. The winter monsoon induced productivity in the northwest Arabian sea showed a strong 100 kyr periodicity as well (Almogi-Labin et al., 2000).

The productivity proxy shows a good correlation with both eccentricity and precession cycles (Figure 5). Many studies from the Arabian Sea have reported the 23 kyr precession cycle to be dominant in monsoon induced productivity changes (Prell, 1984; Clemens et al., 1991; Murray and Prell, 1991; Steens et al., 1992; Anderson and Prell, 1993; Beaufort, 1996; Rostek et al., 1997; Reichart et al., 1998; Almogi-Labin et al., 2000; Prabhu and Shankar, 2005). However, this study indicates control of both the 23 kyr and 100 kyr periodicity on the productivity, which suggests that in the long term, the productivity in the Bay of Bengal is affected by both the summer and winter monsoon. Though, as discussed in the previous section, a bulk of the productivity in the Bay of Bengal is controlled by the summer monsoon, the winter monsoon also has considerable control during the stadial periods, specifically when the summer monsoon is weak.

In both the wavelet and spectral analysis, we do not see any distinct transition from 41 kyr periodicity to the 100 kyr periodicity in either the monsoon or productivity (Figures 4 and 5). The 41 kyr periodicity is entirely absent in the winter monsoon assemblage and only present for a short interval during the post-MPT period in the summer monsoon assemblage. However, there is an increase in the significance of 100 kyr periodicity in all the proxies during the post-MPT period. This along with the presence of 41 kyr periodicity in the SMA during the pre-MPT period, albeit less significant, indicates a strengthened 100 kyr cycle post-MPT. The presence of 100 kyr periodicity in all the proxies prior to 925 ka suggests that the 41 kyr to 100 kyr cyclicity change might have a much earlier effect on the Indian monsoon system.

### **5.5 Internal and external forcing of the Indian summer monsoon**

The U1446 record shows a large change after MIS 22. There is a notable shift in the  $\delta^{18}\text{O}$  value of *G. ruber*. All the productivity indicators show a distinct change (Figure 8). The relative abundance of the SMA increased, suggesting a stronger summer monsoon (Figure 6). All these proxies align with intensity and prominence and create a visible boundary in the timeline before and after MIS 22. The continued global effects associated with the MPT caused a major ice sheet expansion, which



generated conditions to cross the threshold to establish 100 kyr glacial-interglacial cycles (Gildor and Tziperman, 2000; Hönisch et al., 2009; Elderfield et al., 2012; Pena and Goldstein, 2014). The visible changes in the climatic proxies discussed here give ample evidence that the signatures of the global change during the MPT are also visible in the Bay of Bengal. These changes in the glacial-interglacial periodicity, that is, earth's internal forcing, have significant control over the Indian monsoon system. The SMA and the *G. bulloides* (%) show a distinct similarity with the  $\delta^{18}\text{O}$  *G. ruber* (Clemens et al., 2021) after MIS 22, which is not present prior to that. This shift suggests that the global ice volume changes have more control over the ISM in the post-MPT period. The ISM in the pre-MPT period might have been controlled by many phenomena and not respond linearly to the ice volume changes. McGrath et al. (2021), from their precipitation isotope record from the same Site U1446, have reported a strong internal forcing on the ISM in the last 640 kyr, that is, the post MPT period.

During the last 1.45 myr, a few intervals are unique in view of the large climatic shift, as compared to other transitions. One such interval was MIS 12, with a consistently strong winter monsoon. However, there was not a large change in insolation and precession forcing during this time (Imbrie and Imbrie, 1980; Raymo, 1997). Therefore, the prominent monsoon shift during MIS 12 was driven by the earth's internal forcing. The high latitudinal processes strongly affect the Indian monsoon (Borah et al., 2020). During MIS 12, the polar front migrated farther south as compared to the last glacial maximum due to the large ice volume (Poli et al., 2000; Billups et al., 2006), thus affecting the global climate (Naafs et al., 2014). The Atlantic Meridional Overturning Circulation (AMOC) stopped completely (Poli et al., 2000). The AMOC shutdown affected the Hadley cell and shifted the ITCZ farther south (Mohtadi et al., 2016), resulting in a highly strengthened winter monsoon. In the late Quaternary records of the Arabian Sea, the shift in winter monsoon intensity has also been linked to the North Atlantic cooling (Mohtadi et al., 2010; Godad et al., 2021). The southward shifting of ITCZ and its subsequent weakening will weaken the ISM (Mohtadi et al., 2014). The lower SST in the Indian Ocean caused by the increased Northern Hemisphere ice volume also reduces the evaporative moisture content of the ITCZ and causes less rainfall in the Indian subcontinent (Stager et al., 2011; Pausata et al., 2011; Tierney et al., 2016). Almogi-Labin et al. (2000) also reported a strong winter monsoon during the MIS 12.

## **6. Conclusion**

The temporal variation in the relative abundance of the planktic foraminifera is used to understand the shift in the Indian summer and winter monsoon in response to the mid-Pleistocene Transition. From the relative abundance of *G. bulloides*, we conclude that although the upwelling intensified

during the interstadials compared to stadials, its intensity in the Bay of Bengal was independent of the strength of the interstadials. The planktic foraminiferal assemblage data (*G. bulloides*, *G. siphonifera*, *T. sacculifer* and *N. dutertrei* as the summer monsoon assemblage and *G. ruber*, *G. menardii* and *G. falconensis* as the winter monsoon assemblage) further confirms that the Indian summer monsoon was stronger during the interstadials. In contrast, the winter monsoon was stronger during the stadials and vice versa. We also demonstrate that the Indian monsoon strongly responded to the MPT. During the pre-MPT period, the ISM was weak. The ISM started strengthening during MIS 24-22 because of the increased cross-equatorial pressure gradient between the southern subtropical Indian Ocean and the Indian subcontinent due to the expansion of Antarctic ice sheets. A large-scale re-organization of the Indian monsoon system is observed after the mid-Pleistocene Transition. Overall, the summer monsoon continued to strengthen after MIS 22 until the present. The winter monsoon was strong during the pre-MPT period. It followed a similar trend as the summer monsoon until MIS 18, after which they showed an opposite variability. The southward migration of the ITCZ due to the shutdown of the AMOC caused a highly strengthened winter monsoon during MIS 12. However, post-MIS 12, the winter monsoon continued to decrease in strength until the present. From the variation in the eutrophic (*G. glutinata*, *G. bulloides*, *G. falconensis* and *N. dutertrei*) and oligotrophic (*G. ruber*, *T. sacculifer* and *G. conglobatus*) assemblages, we infer that the productivity increased during the interstadials, due to the increased nutrient availability because of the strengthened summer monsoon. The productivity in the western Bay of Bengal also increased during the post MPT period. During the post MPT period, the winter monsoon was mainly controlled by the eccentricity forcing. However, the summer monsoon was more affected by the precession cycle.

### **Data availability**

The data associated with this paper has been provided as supplementary material. It can be accessed in the online version of this article. The data presented here will also be uploaded to PANGAEA.

### **Acknowledgements**

We thank the International Ocean Discovery Program for providing the samples of Site IODP353 U1446. The authors also thank Dr. Dinesh Kumar Naik, Banaras Hindu University, for participating in Expedition 353 and obtaining the samples. The authors thank the Director, National Institute of Oceanography, Goa, India, for the infrastructural support and permission to publish the findings. The authors acknowledge the financial support from the Council of Scientific and Industrial Research for the LEMAP project. We thank Dr. Antje Voelker, Editor, Quaternary Science Reviews, and two

anonymous reviewers for their extensive comments and suggestions that helped us to improve the manuscript.

## Reference

- Ahmad, S.M., Babu, G.A., Padmakumari, V.M. and Raza, W., 2008. Surface and deep water changes in the northeast Indian Ocean during the last 60 ka inferred from carbon and oxygen isotopes of planktonic and benthic foraminifera. *Palaeogeography, Palaeoclimatology, Palaeoecology*, 262, pp.182-188.
- Almogi-Labin, A., Schmiedl, G., Hemleben, C., Siman-Tov, R., Segl, M. and Meischner, D., 2000. The influence of the NE winter monsoon on productivity changes in the Gulf of Aden, NW Arabian Sea, during the last 530 ka as recorded by foraminifera. *Marine Micropaleontology*, 40, pp.295-319.
- Alonso-Garcia, M., Rodrigues, T., Abrantes, F., Padilha, M., Alvarez-Zarikian, C.A., Kunkelova, T., Wright, J.D. and Betzler, C., 2019. Sea-surface temperature, productivity and hydrological changes in the Northern Indian Ocean (Maldives) during the interval~ 575-175 ka (MIS 14 to 7). *Palaeogeography, Palaeoclimatology, Palaeoecology*, 536, p.109376.
- Alvarez Zarikian, C.A., Nadiri, C., Alonso-García, M., Rodrigues, T., Huang, H.-H.M., Lindhorst, S., Kunkelova, T., Kroon, D., Betzler, C., Yasuhara, M., 2022. Ostracod response to monsoon and OMZ variability over the past 1.2 Myr. *Marine Micropaleontology*, 174, 102105.
- An, Z.S., Liu, T.S., Lu, Y.C., Porter, S.C., Kukla, G.J., Wu, X.H., Hua, Y.M., 1990. The long-term paleomonsoon variation recorded by the loess–paleosol sequence in central China. *Quaternary International*, 7, pp.91–95.
- Anderson, D.M. and Prell, W.L., 1992. The structure of the southwest monsoon winds over the Arabian Sea during the late Quaternary: Observations, simulations, and marine geologic evidence. *Journal of Geophysical Research: Oceans*, 97, pp.15481-15487.
- Anderson, D.M. and Prell, W.L., 1993. A 300 kyr record of upwelling off Oman during the late Quaternary: evidence of the Asian southwest monsoon. *Paleoceanography*, 8, pp.193-208.
- Ashfaq, M., Shi, Y., Tung, W.W., Trapp, R.J., Gao, X., Pal, J.S. and Diffenbaugh, N.S., 2009. Suppression of south Asian summer monsoon precipitation in the 21st century. *Geophysical Research Letters*, 36, p. L01704.
- Balachandran, K.K., Laluraj, C.M., Jyothibabu, R., Madhu, N.V., Muraleedharan, K.R., Vijay, J.G., Maheswaran, P.A., Ashraff, T.M., Nair, K.K.C. and Achuthankutty, C.T., 2008. Hydrography and biogeochemistry of the north western Bay of Bengal and the north eastern Arabian Sea during winter monsoon. *Journal of Marine Systems*, 73, pp.76-86.
- Bassinot, F.C., Beaufort, L., Vincent, E., Labeyrie, L.D., Rostek, F., Müller, P.J., Quidelleur, X. and Lancelot, Y., 1994. Coarse fraction fluctuations in pelagic carbonate sediments from the tropical Indian Ocean: A 1500-kyr record of carbonate dissolution. *Paleoceanography*, 9, pp.579-600.
- Bé, A.W. and Hutson, W.H., 1977. Ecology of planktonic foraminifera and biogeographic patterns of life and fossil assemblages in the Indian Ocean. *Micropaleontology*, 23, pp.369-414.

- Beaufort, L., 1996. Dynamics of the monsoon in the equatorial Indian Ocean over the last 260,000 years. *Quaternary International*, 31, pp.13-18.
- Berger, A. and Loutre, M.F., 1991. Insolation values for the climate of the last 10 million years. *Quaternary Science Reviews*, 10, pp.297-317.
- Berger, W.H., Smetacek, V.S., Wefer, G., 1989. Ocean productivity and paleoproductivity - an overview. *Productivity of the Ocean: Present and Past*. John Wiley and Sons, pp. 1–34.
- Bhadra, S.R. and Saraswat, R., 2021. Assessing the effect of riverine discharge on planktic foraminifera: A case study from the marginal marine regions of the western Bay of Bengal. *Deep Sea Research Part II: Topical Studies in Oceanography*, 183, p.104927.
- Billups, K., Lindley, C., Fislser, J. and Martin, P., 2006. Mid Pleistocene climate instability in the subtropical northwestern Atlantic. *Global and planetary change*, 54, pp.251-262.
- Borah, P.J., Venugopal, V., Sukhatme, J., Muddebihal, P., Goswami, B.N. 2020. Indian monsoon derailed by a North Atlantic wavetrain. *Science*, 370, pp. 1335-1338.
- Bosmans, J.H.C., Erb, M.P., Dolan, A.M., Drijfhout, S.S., Tuenter, E., Hilgen, F.J., Edge, D., Pope, J.O. and Lourens, L.J., 2018. Response of the Asian summer monsoons to idealized precession and obliquity forcing in a set of GCMs. *Quaternary Science Reviews*, 188, pp.121-135.
- Broecker, W.S., 1982. Ocean chemistry during glacial time. *Geochimica et Cosmochimica Acta*, 46, pp.1689-1705.
- Cai, Y., Fung, I.Y., Edwards, R.L., An, Z., Cheng, H., Lee, J.E., Tan, L., Shen, C.C., Wang, X., Day, J.A. and Zhou, W., 2015. Variability of stalagmite-inferred Indian monsoon precipitation over the past 252,000 y. *Proceedings of the National Academy of Sciences*, 112, pp.2954-2959.
- Caley, T., Malaizé, B., Revel, M., Ducassou, E., Wainer, K., Ibrahim, M., Shoaib, D., Migeon, S. and Marieu, V., 2011. Orbital timing of the Indian, East Asian and African boreal monsoons and the concept of a 'global monsoon'. *Quaternary Science Reviews*, 30, pp.3705-3715.
- Chaitanya, A.V.S., Lengaigne, M., Vialard, J., Gopalakrishna, V.V., Durand, F., Kranthikumar, C., Amritash, S., Suneel, V., Papa, F. and Ravichandran, M., 2014. Salinity measurements collected by fishermen reveal a “river in the sea” flowing along the eastern coast of India. *Bulletin of the American Meteorological Society*, 95, pp.1897-1908.
- Chapman, M.R., 2010. Seasonal production patterns of planktonic foraminifera in the NE Atlantic Ocean: Implications for paleotemperature and hydrographic reconstructions. *Paleoceanography*, 25, p. PA1101.
- Chappellaz, J., Blunier, T., Raynaud, D., Barnola, J.M., Schwander, J. and Stauffert, B., 1993. Synchronous changes in atmospheric CH<sub>4</sub> and Greenland climate between 40 and 8 kyr BP. *Nature*, 366, pp.443-445.
- Chen, H., Xu, Z., Clift, P.D., Lim, D., Khim, B.K. and Yu, Z., 2019. Orbital-scale evolution of the Indian summer monsoon since 1.2 Ma: evidence from clay mineral records at IODP Expedition 355 Site U1456 in the eastern Arabian Sea. *Journal of Asian Earth Sciences*, 174, pp.11-22.

- Chen, H., Xu, Z., Lim, D., Clift, P.D., Chang, F., Li, T., Cai, M., Wang, W., Yu, Z. and Sun, R., 2020. Geochemical records of the provenance and silicate weathering/erosion from the eastern Arabian Sea and their responses to the Indian summer monsoon since the Mid-Pleistocene. *Paleoceanography and Paleoclimatology*, 35, p. e2019PA003732.
- Clark, P.U., Archer, D., Pollard, D., Blum, J.D., Rial, J.A., Brovkin, V., Mix, A.C., Pisias, N.G. and Roy, M., 2006. The middle Pleistocene transition: characteristics, mechanisms, and implications for long-term changes in atmospheric pCO<sub>2</sub>. *Quaternary Science Reviews*, 25, pp.3150-3184.
- Clemens, S., Prell, W., Murray, D., Shimmield, G. and Weedon, G., 1991. Forcing mechanisms of the Indian Ocean monsoon. *Nature*, 353, pp.720-725.
- Clemens, S.C., Murray, D.W. and Prell, W.L., 1996. Nonstationary phase of the Plio-Pleistocene Asian monsoon. *Science*, 274, pp.943-948.
- Clemens, S.C. and Prell, W.L., 2003. A 350,000 year summer-monsoon multi-proxy stack from the Owen Ridge, Northern Arabian Sea. *Marine Geology*, 201, pp.35-51.
- Clemens, S.C., Kuhnt, W., LeVay, L.J., Anand, P., Ando, T., Bartol, M., Bolton, C.T., Ding, X., Gariboldi, K., Giosan, L., Hathorne, E.C., Huang, Y., Jaiswal, P., Kim, S., Kirkpatrick, J.B., Littler, K., Marino, G., Martinez, P., Naik, D., Peketi, A., Phillips, S.C., Robinson, M.M., Romero, O.E., Sagar, N., Taladay, K.B., Taylor, S.N., Thirumalai, K., Uramoto, G., Usui, Y., Wang, J., Yamamoto, M., and Zhou, L., 2016. Site U1446. In Clemens, S.C., Kuhnt, W., LeVay, L.J., and the Expedition 353 Scientists, Indian Monsoon Rainfall. *Proceedings of the International Ocean Discovery Program*, 353.
- Clemens, S.C., Yamamoto, M., Thirumalai, K., Giosan, L., Richey, J.N., Nilsson-Kerr, K., Rosenthal, Y., Anand, P. and McGrath, S.M., 2021. Remote and local drivers of Pleistocene South Asian summer monsoon precipitation: A test for future predictions. *Science Advances*, 7, p. eabg3848.
- Colin, C., Kissel, C., Blamart, D., Turpin, L., 1998. Magnetic properties of sediments in the Bay of Bengal and the Andaman Sea: impact of rapid North Atlantic Ocean climatic events on the strength of the Indian monsoon. *Earth and Planetary Science Letters*, 160, pp.623-635.
- Conan, S.H. and Brummer, G.J.A., 2000. Fluxes of planktic foraminifera in response to monsoonal upwelling on the Somalia Basin margin. *Deep Sea Research Part II: Topical Studies in Oceanography*, 47, pp.2207-2227.
- Cullen, J.L. and Prell, W.L., 1984. Planktonic foraminifera of the northern Indian Ocean: distribution and preservation in surface sediments. *Marine Micropaleontology*, 9, pp.1-52.
- Curry, W.B., Ostermann, D.R., Guptha, M.V.S. and Ittekkot, V., 1992. Foraminiferal production and monsoonal upwelling in the Arabian Sea: evidence from sediment traps. *Geological Society, London, Special Publications*, 64, pp.93-106.
- de Noblet, N., Braconnot, P., Joussaume, S. and Masson, V., 1996. Sensitivity of simulated Asian and African summer monsoons to orbitally induced variations in insolation 126, 115 and 6 kBP. *Climate Dynamics*, 12, pp.589-603.
- Demencol, P.B., 1995. Plio-pleistocene African climate. *Science*, 270, pp.53-59.

- Detlef, H., Belt, S.T., Sosdian, S.M., Smik, L., Lear, C.H., Hall, I.R., Cabedo-Sanz, P., Husum, K. and Kender, S., 2018. Sea ice dynamics across the Mid-Pleistocene transition in the Bering Sea. *Nature communications*, 9, pp.1-11.
- Ding, Z., Liu, T., Rutter, N.W., Yu, Z., Guo, Z. and Zhu, R., 1995. Ice-volume forcing of East Asian winter monsoon variations in the past 800,000 years. *Quaternary Research*, 44, pp.149-159.
- Duplessy, J.C., 1982. Glacial to Interglacial contrast in the northern Indian Ocean. *Nature*, 295, pp.494-498.
- Elderfield, H., Ferretti, P., Greaves, M., Crowhurst, S., McCave, I.N., Hodell, D. and Piotrowski, A.M., 2012. Evolution of ocean temperature and ice volume through the mid-Pleistocene climate transition. *Science*, 337, pp.704-709.
- Emeis, K.C., Anderson, D.M., Dooe, H., Kroon, D. and Schulz-Bull, D., 1995. Sea-surface temperatures and the history of monsoon upwelling in the northwest Arabian Sea during the last 500,000 years. *Quaternary Research*, 43, pp.355-361.
- Farmer, J.R., Hönisch, B., Haynes, L.L., Kroon, D., Jung, S., Ford, H.L., Raymo, M.E., Jaume-Seguí, M., Bell, D.B., Goldstein, S.L. and Pena, L.D., 2019. Deep Atlantic Ocean carbon storage and the rise of 100,000-year glacial cycles. *Nature Geoscience*, 12, pp.355-360.
- Fasullo, J. and Webster, P.J., 2003. A hydrological definition of Indian monsoon onset and withdrawal. *Journal of Climate*, 16, pp.3200-3211.
- Gadgil, S., 2003. The Indian monsoon and its variability. *Annual Review of Earth and Planetary Sciences*, 31, pp.429-467.
- Gadgil, S., Rajeevan, M. and Francis, P.A., 2007. Monsoon variability: Links to major oscillations over the equatorial Pacific and Indian oceans. *Current Science*, 93, pp.182-194.
- Gildor, H. and Tziperman, E., 2000. Sea ice as the glacial cycles' climate switch: Role of seasonal and orbital forcing. *Paleoceanography*, 15, pp.605-615.
- Godad, S.P., Panmei, C. and Naidu, P.D., 2021. Remote forcing of winter cooling in the Arabian Sea: Implications for the NE monsoon. *Palaeogeography, Palaeoclimatology, Palaeoecology*, 586, p.110755.
- Govil, P., Naidu, P.D., 2011. Variations of Indian monsoon precipitation during the last 32 kyr reflected in the surface hydrography of the western Bay of Bengal. *Quaternary Science Reviews*, 30, pp.3871-3879.
- Guo, Z., Biscaye, P., Wei, L., Chen, X., Peng, S. and Liu, T., 2000. Summer monsoon variations over the last 1.2 Ma from the weathering of loess-soil sequences in China. *Geophysical Research Letters*, 27, pp.1751-1754.
- Guo, Z.T., Berger, A., Yin, Q.Z. and Qin, L., 2009. Strong asymmetry of hemispheric climates during MIS-13 inferred from correlating China loess and Antarctica ice records. *Climate of the Past*, 5, pp.21-31.
- Guo, Z., Zhou, X. and Wu, H., 2012. Glacial-interglacial water cycle, global monsoon and atmospheric methane changes. *Climate Dynamics*, 39, pp.1073-1092.

- Gupta, A.K., Anderson, D.M., Overpeck, J.T., 2003. Abrupt changes in the Asian southwest monsoon during the Holocene and their links to the North Atlantic Ocean. *Nature*, 421, pp.354–357
- Gupta, A.K., Sarkar, S., De, S., Clemens, S.C. and Velu, A., 2010. Mid-Brunhes strengthening of the Indian Ocean Dipole caused increased equatorial East African and decreased Australasian rainfall. *Geophysical Research Letters*, 37, p. L06706.
- Guptha, M.V.S., Curry, W.B., Ittekkot, V., Muralinath, A.S., 1997. Seasonal variation in the flux of planktic Foraminifera; sediment trap results from the Bay of Bengal, northern Indian Ocean. *Journal of Foraminiferal Research*, 27, pp.5–19.
- Hammer, Ø., Harper, D.A. and Ryan, P.D., 2001. PAST: Paleontological statistics software package for education and data analysis. *Palaeontologia electronica*, 4, p.9.
- Hao, Q., Wang, L., Oldfield, F. and Guo, Z., 2015. Extra-long interglacial in Northern Hemisphere during MISs 15-13 arising from limited extent of Arctic ice sheets in glacial MIS 14. *Scientific Reports*, 5, pp.1-8.
- Hastenrath, S., Nicklis, A. and Greischar, L., 1993. Atmospheric-hydrospheric mechanisms of climate anomalies in the western equatorial Indian Ocean. *Journal of Geophysical Research: Oceans*, 98, pp.20219-20235.
- Hearty, P.J., Kindler, P., Cheng, H. and Edwards, R.L., 1999. A + 20 m middle Pleistocene sea-level highstand (Bermuda and the Bahamas) due to partial collapse of Antarctic ice. *Geology*, 27, pp.375-378.
- Helber, R.W., Kara, A.B., Richman, J.G., Carnes, M.R., Barron, C.N., Hurlburt, H.E. and Boyer, T., 2012. Temperature versus salinity gradients below the ocean mixed layer. *Journal of Geophysical Research: Oceans*, 117, p. C05006.
- Hemleben, C., Spindler, M. and Anderson, O.R., 2012. *Modern planktonic foraminifera*. Springer Science & Business Media.
- Herbert, T.D., Peterson, L.C., Lawrence, K.T. and Liu, Z., 2010. Tropical ocean temperatures over the past 3.5 million years. *science*, 328, pp.1530-1534.
- Herguera, J.C., Berger, W.H., 1991. Paleoproductivity: glacial to postglacial change in the western equatorial Pacific from benthic foraminifera. *Geology*, 19, pp.1173–1176.
- Hollstein, M., Mohtadi, M., Rosenthal, Y., Moffa Sanchez, P., Oppo, D., Martínez Méndez, G., Steinke, S. and Hebbeln, D., 2017. Stable oxygen isotopes and Mg/Ca in planktic foraminifera from modern surface sediments of the Western Pacific Warm Pool: Implications for thermocline reconstructions. *Paleoceanography*, 32, pp.1174-1194.
- Hönisch, B., Hemming, N.G., Archer, D., Siddall, M. and McManus, J.F., 2009. Atmospheric carbon dioxide concentration across the mid-Pleistocene transition. *Science*, 324, pp.1551-1554.
- Imbrie, J. and Imbrie, J.Z., 1980. Modeling the climatic response to orbital variations. *Science*, 207, pp.943-953.

- Imbrie, J., Boyle, E.A., Clemens, S.C., Duffy, A., Howard, W.R., Kukla, G., Kutzbach, J., Martinson, D.G., McIntyre, A., Mix, A.C. and Molino, B., 1992. On the structure and origin of major glacial cycles 1. Linear responses to Milankovitch forcing. *Paleoceanography*, 7, pp.701-738.
- Ivanova, E., Schiebel, R., Singh, A.D., Schmiedl, G., Niebler, H.S. and Hemleben, C., 2003. Primary production in the Arabian Sea during the last 135 000 years. *Palaeogeography, Palaeoclimatology, Palaeoecology*, 197, pp.61-82.
- Jiang, F., Zhu, X., Li, T., Zhou, Y., Xiong, Z., Feng, X., Yin, X. and Li, A., 2019. Increased dust deposition in the Parece Vela Basin since the mid-Pleistocene inferred from radiogenic Sr and Nd isotopes. *Global and Planetary Change*, 173, pp.83-95.
- Jouzel, J., Masson-Delmotte, V., Cattani, O., Dreyfus, G., Falourd, S., Hoffmann, G., Minster, B., Nouet, J., Barnola, J.M., Chappellaz, J. and Fischer, H., 2007. Orbital and millennial Antarctic climate variability over the past 800,000 years. *science*, 317, pp.793-796.
- Kathayat, G., Cheng, H., Sinha, A., Spötl, C., Edwards, R.L., Zhang, H., Li, X., Yi, L., Ning, Y., Cai, Y. and Lui, W.L., 2016. Indian monsoon variability on millennial-orbital timescales. *Scientific reports*, 6, pp.1-7.
- Kender, S., Ravelo, A.C., Worne, S., Swann, G.E., Leng, M.J., Asahi, H., Becker, J., Detlef, H., Aiello, I.W., Andreasen, D. and Hall, I.R., 2018. Closure of the Bering Strait caused mid-Pleistocene transition cooling. *Nature communications*, 9, pp.1-11.
- Kitoh, A., Yukimoto, S., Noda, A. and Motoi, T., 1997. Simulated changes in the Asian summer monsoon at times of increased atmospheric CO<sub>2</sub>. *Journal of the Meteorological Society of Japan*. Ser. II, 75, pp.1019-1031.
- Kitoh, A., Endo, H., Krishna Kumar, K., Cavalcanti, I.F., Goswami, P. and Zhou, T., 2013. Monsoons in a changing world: A regional perspective in a global context. *Journal of Geophysical Research: Atmospheres*, 118, pp.3053-3065.
- Koutsodendris, A., Sachse, D., Appel, E., Herb, C., Fischer, T., Fang, X. and Pross, J., 2018. Prolonged monsoonal moisture availability preconditioned glaciation of the Tibetan Plateau during the Mid-Pleistocene Transition. *Geophysical Research Letters*, 45, pp.13-020.
- Krishnamurti, T.N., 1985. Summer monsoon experiment—A review. *Monthly Weather Review*, 113, pp.1590-1626.
- Kudrass, H.R., Hofmann, A., Dose, H., Emeis, K., Erlenkeuser, H., 2001. Modulation and amplification of climatic changes in the Northern Hemisphere by the Indian summer monsoon during the past 80 k.y. *Geology*, 29, pp.63-66.
- Kunkelova, T., Jung, S.J., De Leau, E.S., Odling, N., Thomas, A.L., Betzler, C., Eberli, G.P., Alvarez-Zarikian, C.A., Alonso-García, M., Bialik, O.M. and Blättler, C.L., 2018. A two million year record of low-latitude aridity linked to continental weathering from the Maldives. *Progress in Earth and Planetary Science*, 5, pp.1-20.
- Kutzbach, J.E., 1981. Monsoon climate of the early Holocene: climate experiment with the earth's orbital parameters for 9000 years ago. *Science*, 214, pp.59-61.



- Kutzbach, J.E. and Guetter, P.J., 1986. The influence of changing orbital parameters and surface boundary conditions on climate simulations for the past 18 000 years. *Journal of atmospheric sciences*, 43, pp.1726-1759.
- Lange, C.B., 1993. Diatom productivity and preservation in the western equatorial Pacific: the Quaternary record. In *Proceedings of . ODP Scientific Results*, 30, pp. 509-523.
- Lauterbach, S., Andersen, N., Wang, Y.V., Blanz, T., Larsen, T. and Schneider, R.R., 2020. An~ 130 kyr record of surface water temperature and  $\delta^{18}O$  from the northern Bay of Bengal: Investigating the linkage between Heinrich events and Weak Monsoon Intervals in Asia. *Paleoceanography and Paleoclimatology*, 35, p. e2019PA003646.
- Lee, J.Y. and Wang, B., 2014. Future change of global monsoon in the CMIP5. *Climate Dynamics*, 42, pp.101-119.
- Lee, J., Kim, S. and Khim, BK, 2020. A paleoproductivity shift in the northwestern Bay of Bengal (IODP Site U1445) across the Mid-Pleistocene transition in response to weakening of the Indian summer monsoon. *Palaeogeography, Palaeoclimatology, Palaeoecology*, 560, pp.110018.
- Lisiecki, L.E. and Raymo, M.E., 2005. A Pliocene-Pleistocene stack of 57 globally distributed benthic  $\delta^{18}O$  records. *Paleoceanography*, 20, p. PA1003.
- Liu, X., Liu, Z., Kutzbach, J.E., Clemens, S.C. and Prell, W.L., 2006. Hemispheric insolation forcing of the Indian Ocean and Asian monsoon: local versus remote impacts. *Journal of Climate*, 19, pp.6195-6208.
- Locarnini, M., Mishonov, A.V., Baranova, O.K., Boyer, T.P., Zweng, M.M., Garcia, H.E., Seidov, D., Weathers, K., Paver, C. and Smolyar, I., 2018. World ocean atlas 2018, volume 1: Temperature. In: A. Mishonov, Technical Editor. NOAA Atlas NESDIS, 81, pp. 52.
- Loulergue, L., Schilt, A., Spahni, R., Masson-Delmotte, V., Blunier, T., Lemieux, B., Barnola, J.M., Raynaud, D., Stocker, T.F. and Chappellaz, J., 2008. Orbital and millennial-scale features of atmospheric CH<sub>4</sub> over the past 800,000 years. *Nature*, 453, pp.383-386.
- Lüthi, D., Le Floch, M., Bereiter, B., Blunier, T., Barnola, J.M., Siegenthaler, U., Raynaud, D., Jouzel, J., Fischer, H., Kawamura, K. and Stocker, T.F., 2008. High-resolution carbon dioxide concentration record 650,000–800,000 years before present. *Nature*, 453, pp.379-382.
- Madhupratap, M., Gauns, M., Ramaiah, N., Kumar, S.P., Muraleedharan, P.M., De Sousa, S.N., Sardesai, S. and Muraleedharan, U., 2003. Biogeochemistry of the Bay of Bengal: physical, chemical and primary productivity characteristics of the central and western Bay of Bengal during summer monsoon 2001. *Deep Sea Research Part II: Topical Studies in Oceanography*, 50, pp.881-896.
- Martínez-García, A., Rosell-Melé, A., Jaccard, S.L., Geibert, W., Sigman, D.M. and Haug, G.H., 2011. Southern Ocean dust–climate coupling over the past four million years. *Nature*, 476, pp.312-315.
- Maslin, M.A., Li, X.S., Loutre, M.F. and Berger, A., 1998. The contribution of orbital forcing to the progressive intensification of Northern Hemisphere glaciation. *Quaternary Science Reviews*, 17, pp.411-426.

- Masson-Delmotte, V., Stenni, B., Pol, K., Braconnot, P., Cattani, O., Falourd, S., Kageyama, M., Jouzel, J., Landais, A., Minster, B. and Barnola, J.M., 2010. EPICA Dome C record of glacial and interglacial intensities. *Quaternary Science Reviews*, 29, pp.113-128.
- May, W., 2004. Simulation of the variability and extremes of daily rainfall during the Indian summer monsoon for present and future times in a global time-slice experiment. *Climate Dynamics*, 22, pp.183-204.
- McGrath, S.M., Clemens, S.C., Huang, Y. and Yamamoto, M., 2021. Greenhouse gas and ice volume drive pleistoceneindian summer monsoon precipitation isotope variability. *Geophysical Research Letters*, 48, p.e2020GL092249.
- McClymont, E.L., Sostdian, S.M., Rosell-Melé, A. and Rosenthal, Y., 2013. Pleistocene sea-surface temperature evolution: Early cooling, delayed glacial intensification, and implications for the mid-Pleistocene climate transition. *Earth-Science Reviews*, 123, pp.173-193.
- Meehl, G.A., 1997. The south Asian monsoon and the tropospheric biennial oscillation. *Journal of Climate*, 10, pp.1921-1943.
- Meehl, G.A. and Arblaster, J.M., 2003. Mechanisms for projected future changes in south Asian monsoon precipitation. *Climate Dynamics*, 21, pp.659-675.
- Miranda, J., Baliarsingh, S.K., Lotliker, A.A., Sahoo, S., Sahu, K.C. and Kumar, T.S., 2020. Long-term trend and environmental determinants of phytoplankton biomass in coastal waters of northwestern Bay of Bengal. *Environmental monitoring and assessment*, 192, pp.1-13.
- Mohan, K. and Gupta, A.K., 2011. Intense deep convective mixing in the southeast Arabian Sea linked to strengthening of the northeast Indian monsoon during the middle Pliocene (3.4 Ma). *Current Science*, 101, pp.1-5.
- Mohtadi, M., Steinke, S., Lückge, A., Groeneveld, J., Hathorne, E.C., 2010. Glacial to Holocene surface hydrography of the tropical eastern Indian Ocean. *Earth Planetary Science Letters*, 292, pp.89–97.
- Mohtadi, M., Prange, M., Oppo, D.W., De Pol-Holz, R., Merkel, U., Zhang, X., Steinke, S. and Lückge, A., 2014. North Atlantic forcing of tropical Indian Ocean climate. *Nature*, 509, pp.76-80.
- Mohtadi, M., Prange, M. and Steinke, S., 2016. Palaeoclimatic insights into forcing and response of monsoon rainfall. *Nature*, 533, pp.191-199.
- Müller, P.J. and Suess, E., 1979. Productivity, sedimentation rate, and sedimentary organic matter in the oceans—I. Organic carbon preservation. *Deep Sea Research Part A. Oceanographic Research Papers*, 26, pp.1347-1362.
- Munz, P.M., Siccha, M., Lückge, A., Böll, A., Kucera, M. and Schulz, H., 2015. Decadal-resolution record of winter monsoon intensity over the last two millennia from planktic foraminiferal assemblages in the northeastern Arabian Sea. *The Holocene*, 25, pp.1756-1771.
- Muraleedharan, K.R., Jasmine, P., Achuthankutty, C.T., Revichandran, C., Kumar, P.D., Anand, P. and Rejomon, G., 2007. Influence of basin-scale and mesoscale physical processes on biological productivity in the Bay of Bengal during the summer monsoon. *Progress in Oceanography*, 72, pp.364-383.

- Murray, D.W., Prell, W.L., 1991. Pliocene to Pleistocene variations in calcium carbonate, organic carbon, and opal on the Owen Ridge, northern Arabian Sea. *Proceedings of the Ocean Drilling Program, Scientific Results*, 117, 343–363.
- Naafs, B.D.A., Hefter, J. and Stein, R., 2014. Dansgaard-Oeschger forcing of sea surface temperature variability in the midlatitude North Atlantic between 500 and 400 ka (MIS 12). *Paleoceanography*, 29, pp.1024-1030.
- Naik, D.K., Saraswat, R., Lea, D.W., Kurtarkar, S.R., and Mackensen, A. 2017. Last glacial-interglacial productivity and associated changes in the eastern Arabian Sea. *Palaeogeography, Palaeoclimatology, Palaeoecology*, 483, pp. 147-156.
- Nilsson-Kerr, K., Anand, P., Sexton, P.F., Leng, M.J., Misra, S., Clemens, S.C. and Hammond, S.J., 2019. Role of Asian summer monsoon subsystems in the inter-hemispheric progression of deglaciation. *Nature Geoscience*, 12, pp.290-295.
- Oliveira, D., Desprat, S., Yin, Q., Rodrigues, T., Naughton, F., Trigo, R.M., Su, Q., Grimalt, J.O., Alonso-Garcia, M., Voelker, A.H.L., Abrantes, F., Sánchez Goñi, M.F., 2020. Combination of insolation and ice-sheet forcing drive enhanced humidity in northern subtropical regions during MIS 13. *Quaternary Science Reviews*, 247, p.106573.
- Overpeck, J.T., Anderson, D., Trumbore, S., Prell, W., 1996. The southwest Indian monsoon over the last 18, 000 years. *Climate Dynamics*, 12, 213–225.
- Papa, F., S. K. Bala, R. K. Pandey, F. Durand, V. V. Gopalakrishna, A. Rahman, and Rossow, W. B., 2012. Ganga-Brahmaputra river discharge from Jason-2 radar altimetry: An update to the long-term satellite-derived estimates of continental freshwater forcing flux into the Bay of Bengal. *Journal of Geophysical Research*, 117, p. C11021.
- Parker, F.L., 1962. Planktonic foraminiferal species in Pacific sediments. *Micropaleontology*, 8, pp.219-254.
- Pattan, J.N., Masuzawa, T., Naidu, P.D., Parthiban, G. and Yamamoto, M., 2003. Productivity fluctuations in the southeastern Arabian Sea during the last 140 ka. *Palaeogeography, Palaeoclimatology, Palaeoecology*, 193, pp.575-590.
- Paul, J.T., Ramaiah, N. and Sardesai, S., 2008. Nutrient regimes and their effect on distribution of phytoplankton in the Bay of Bengal. *Marine Environmental Research*, 66, pp.337-344.
- Pausata, F.S., Li, C., Wettstein, J.J., Kageyama, M. and Nisancioglu, K.H., 2011. The key role of topography in altering North Atlantic atmospheric circulation during the last glacial period. *Climate of the Past*, 7, pp.1089-1101.
- Peeters, F.J. and Brummer, G.J.A., 2002. The seasonal and vertical distribution of living planktic foraminifera in the NW Arabian Sea. *Geological Society, London, Special Publications*, 195, pp.463-497.
- Pena, L.D. and Goldstein, S.L., 2014. Thermohaline circulation crisis and impacts during the mid-Pleistocene transition. *Science*, 345, pp.318-322.

- Poli, M.S., Thunell, R.C. and Rio, D., 2000. Millennial-scale changes in North Atlantic Deep Water circulation during marine isotope stages 11 and 12: Linkage to Antarctic climate. *Geology*, 28, pp.807-810.
- Prabhu, C.N. and Shankar, R., 2005. Palaeoproductivity of the eastern Arabian Sea during the past 200 ka: A multi-proxy investigation. *Deep Sea Research Part II: Topical Studies in Oceanography*, 52, pp.1994-2002.
- Prasad, T.G., 2004. A comparison of mixed-layer dynamics between the Arabian Sea and Bay of Bengal: One-dimensional model results. *Journal of Geophysical Research: Oceans*, 109, p. C03035.
- Prasanna Kumar, S., Muraleedharan, P.M., Prasad, T.G., Gauns, M., Ramaiah, N., De Souza, S.N., Sardesai, S. and Madhupratap, M., 2002. Why is the Bay of Bengal less productive during summer monsoon compared to the Arabian Sea?. *Geophysical Research Letters*, 29, pp.88-1.
- Prasanna Kumar, S., Nuncio, M., Narvekar, J., Kumar, A., Sardesai, D.S., De Souza, S.N., Gauns, M., Ramaiah, N. and Madhupratap, M., 2004. Are eddies nature's trigger to enhance biological productivity in the Bay of Bengal?. *Geophysical Research Letters*, 31, p. L07309.
- Prell, W.L. and Curry, W.B., 1981. Faunal and isotopic indices of monsoonal upwelling-western arabian sea. *Oceanologica acta*, 4, pp.91-98.
- Prell, W.L., 1984. Variation of monsoonal upwelling: a response to changing solar radiation. *Climate processes and climate sensitivity*, 29, pp.48-57.
- Prell, W.L. and Van Campo, E., 1986. Coherent response of Arabian Sea upwelling and pollen transport to late Quaternary monsoonal winds. *Nature*, 323, pp.526-528.
- Prell, W.L. and Kutzbach, J.E., 1987. Monsoon variability over the past 150,000 years. *Journal of Geophysical Research: Atmospheres*, 92, pp.8411-8425.
- Prokopenko, A.A., Hinnov, L.A., Williams, D.F. and Kuzmin, M.I., 2006. Orbital forcing of continental climate during the Pleistocene: a complete astronomically tuned climatic record from Lake Baikal, SE Siberia. *Quaternary Science Reviews*, 25, pp.3431-3457.
- Railsback, L.B., Gibbard, P.L., Head, M.J., Voarintsoa, N.R.G. and Toucanne, S., 2015. An optimized scheme of lettered marine isotope substages for the last 1.0 million years, and the climatostratigraphic nature of isotope stages and substages. *Quaternary Science Reviews*, 11, pp.94-106.
- Raymo, M.E., 1997. The timing of major climate terminations. *Paleoceanography*, 12, pp.577-585.
- Raymo, M.E., Lisiecki, L.E. and Nisancioglu, K.H., 2006. Plio-Pleistocene ice volume, Antarctic climate, and the global  $\delta^{18}\text{O}$  record. *Science*, 313, pp.492-495.
- Reichart, G.J., Lournes, L.J., Zachariasse, W.J., 1998. Temporal variability in the northern Arabian Sea Oxygen Minimum Zone (OMZ) during the last 225,000 years. *Paleoceanography*, 13, pp.607-621.

- Rohling, E.J., Foster, G.L., Grant, K.M., Marino, G., Roberts, A.P., Tamisiea, M.E. and Williams, F., 2014. Sea-level and deep-sea-temperature variability over the past 5.3 million years. *Nature*, 508, pp.477–482.
- Rostek, F., Bard, E., Beaufort, L., Sonzogni, C. and Ganssen, G., 1997. Sea surface temperature and productivity records for the past 240 kyr in the Arabian Sea. *Deep Sea Research Part II: Topical Studies in Oceanography*, 44, pp.1461-1480.
- Ruddiman, W.F., 2001. *Earth's Climate: past and future*. Macmillan.
- Saalim, S.M., Saraswat, R., Suokhrie, T., Bhadra, S.R., Kurtarkar, S.R. and Nigam, R., 2017. Benthic foraminiferal response to changes in mining pattern: a case study from the Zuari estuary, Goa, India. *Environmental Earth Sciences*, 76, pp.1-10.
- Sabade, S.S., Kulkarni, A. and Kripalani, R.H., 2011. Projected changes in South Asian summer monsoon by multi-model global warming experiments. *Theoretical and Applied Climatology*, 103, pp.543-565.
- Saji, N.H., Goswami, B.N., Vinayachandran, P.N. and Yamagata, T., 1999. A dipole mode in the tropical Indian Ocean. *Nature*, 401, pp.360-363.
- Saraswat, R., 2015. Non-destructive foraminiferal paleoclimatic proxies: a brief insight. *Proc. Indian National Science Academy*, 81, pp.381–395.
- Saraswat, R., Singh, D.P., Lea, D.W., Mackensen, A., Naik, D.K., 2019. Indonesian throughflow controlled the westward extent of the Indo-Pacific Warm Pool during glacial-interglacial intervals. *Global and Planetary Change*, 183, 103031.
- Saraswat, R., Kurtarkar, S.R., Yadav, R., Mackensen, A., Singh, D.P., Bhadra, S., Singh, A.D., Tiwari, M., Prabhukuluskar, S.P., Bhandodkar, S.R. and Pandey, D.K., 2020. Inconsistent change in surface hydrography of the eastern Arabian Sea during the last four glacial–interglacial intervals. *Geological Magazine*, 157, pp.989-1000.
- Sarma, V.V.S.S., Rao, G.D., Viswanadham, R., Sherin, C.K., Salisbury, J., Omand, M.M., Mahedevan, A., Murty, V.S.N., Shroyer, E.L., Baumgartner, M. and Stafford, K.M., 2016. Effects of freshwater stratification on nutrients, dissolved oxygen and phytoplankton in the Bay of Bengal. *Oceanography*, 29, pp.222-231.
- Schiebel, R. and Hemleben, C., 2000. Interannual variability of planktic foraminiferal populations and test flux in the eastern North Atlantic Ocean (JGOFS). *Deep Sea Research Part II: Topical Studies in Oceanography*, 47, pp.1809-1852.
- Schiebel, R., Waniek, J., Bork, M. and Hemleben, C., 2001. Planktic foraminiferal production stimulated by chlorophyll redistribution and entrainment of nutrients. *Deep Sea Research Part I: Oceanographic Research Papers*, 48, pp.721-740.
- Schiebel, R., Zeltner, A., Treppke, U.F., Waniek, J.J., Bollmann, J., Rixen, T., Hemleben, C., 2004. Distribution of diatoms, coccolithophores and planktic foraminifers along a trophic gradient during SW monsoon in the Arabian Sea. *Marine Micropaleontology*, 51, pp.345–371.
- Schiebel, R. and Hemleben, C., 2017. *Planktic foraminifers in the modern ocean*. Berlin: Springer.

- Schott, F.A. and McCreary Jr, J.P., 2001. The monsoon circulation of the Indian Ocean. *Progress in Oceanography*, 51, pp.1-123.
- Schott, F.A., Xie, S.P. and McCreary Jr, J.P., 2009. Indian Ocean circulation and climate variability. *Reviews of Geophysics*, 47, p. RG1002.
- Schulz, H., von Rad, U. and Ittekkot, V., 2002. Planktic foraminifera, particle flux and oceanic productivity off Pakistan, NE Arabian Sea: modern analogues and application to the palaeoclimatic record. *Geological Society, London, Special Publications*, 195, pp.499-516.
- Seears, H.A., F Darling, K., Wade, C.M., 2012. Ecological partitioning and diversity in tropical planktonic foraminifera. *BMC Evolutionary Biology*, 12, p. 54.
- Sengupta, D., Bharath Raj, G.N. and Shenoi, S.S.C., 2006. Surface freshwater from Bay of Bengal runoff and Indonesian throughflow in the tropical Indian Ocean. *Geophysical Research Letters*, 33, p. L22609.
- Seth, A., Rauscher, S.A., Biasutti, M., Giannini, A., Camargo, S.J. and Rojas, M., 2013. CMIP5 projected changes in the annual cycle of precipitation in monsoon regions. *Journal of Climate*, 26, pp.7328-7351.
- Shankar, D., Vinayachandran, P.N., Unnikrishnan, A.S., 2002. The monsoon currents in the north Indian Ocean. *Progress in Oceanography*, 52, pp.63-120.
- Shenoi, S.S.C., Shankar, D. and Shetye, S.R., 2002. Differences in heat budgets of the near-surface Arabian Sea and Bay of Bengal: Implications for the summer monsoon. *Journal of Geophysical Research: Oceans*, 107, pp.5-1.
- Shetye, S.R., Shenoi, S.S.C., Gouveia, A.D., Michael, G.S., Sundar, D. and Nampoothiri, G., 1991. Wind-driven coastal upwelling along the western boundary of the Bay of Bengal during the southwest monsoon. *Continental Shelf Research*, 11, pp.1397-1408.
- Shetye, S.R., 1993. The movement and implications of the Ganges–Brahmaputra runoff on entering the Bay of Bengal. *Current Science*, 64, pp.32-38.
- Shetye, S.R., Gouveia, A.D., Shankar, D., Shenoi, S.S.C., Vinayachandran, P.N., Sundar, D., Michael, G.S. and Nampoothiri, G., 1996. Hydrography and circulation in the western Bay of Bengal during the northeast monsoon. *Journal of Geophysical Research: Oceans*, 101, pp.14011-14025.
- Singh, R.K. and Gupta, A.K., 2005. Systematic decline in benthic foraminiferal species diversity linked to productivity increases over the last 26 Ma in the Indian Ocean. *The Journal of Foraminiferal Research*, 35, pp.219-227.
- Singh, A.D., Kroon, D. and Ganeshram, R.S., 2006. Millennial scale variations in productivity and OMZ intensity in the eastern Arabian Sea. *Journal- Geological Society of India*, 68, p.369.
- Singh, R.K. and Gupta, A.K., 2014. Miocene history of Indian monsoon: A review of marine records. *Indian Miocene: A Geodynamic and chronologic framework for palaeobiota, sedimentary environments and palaeoclimates* (Ed: Tiwari RP) Special Publication of the Palaeontological Society of India, 5, pp.101-109.

- Singh, A.D., Jung, S.J., Anand, P., Kroon, D. and Ganeshram, R.S., 2018. Rapid switch in monsoon-wind induced surface hydrographic conditions of the eastern Arabian Sea during the last deglaciation. *Quaternary International*, 479, pp.3-11.
- Spahni, R., Chappellaz, J., Stocker, T.F., Loulergue, L., Hausammann, G., Kawamura, K., Flückiger, J., Schwander, J., Raynaud, D., Masson-Delmotte, V. and Jouzel, J., 2005. Atmospheric methane and nitrous oxide of the late Pleistocene from Antarctic ice cores. *Science*, 310, pp.1317-1321.
- Stager, J.C., Ryves, D.B., Chase, B.M. and Pausata, F.S., 2011. Catastrophic drought in the Afro-Asian monsoon region during Heinrich event 1. *Science*, 331, pp.1299-1302.
- Steens, T.N., Ganssen, G. and Kroon, D., 1992. Oxygen and carbon isotopes in planktonic foraminifera as indicators of upwelling intensity and upwelling-induced high productivity in sediments from the northwestern Arabian Sea. Geological Society, London, Special Publications, 64, pp.107-119.
- Stoll, H.M., Arevalos, A., Burke, A., Ziveri, P., Mortyn, G., Shimizu, N. and Unger, D., 2007. Seasonal cycles in biogenic production and export in Northern Bay of Bengal sediment traps. *Deep Sea Research Part II: Topical Studies in Oceanography*, 54, pp.558-580.
- Sun, Y., Clemens, S.C., An, Z. and Yu, Z., 2006. Astronomical timescale and palaeoclimatic implication of stacked 3.6-Myr monsoon records from the Chinese Loess Plateau. *Quaternary Science Reviews*, 25, pp.33-48.
- Suokhrie, T., Saalim, S.M., Saraswat, R., and Nigam, R., 2018. Indian monsoon variability in the last 2000 years as inferred from benthic foraminifera. *Quaternary International*, 479, pp. 128-140.
- Suokhrie, T., Saraswat, R., and Saju, S., 2022. Strong solar influence on multi-decadal periodic productivity changes in the central-western Bay of Bengal. *Quaternary International*, 629, pp. 16-26.
- Teitler, L., Florindo, F., Warnke, D.A., Filippelli, G.M., Kupp, G. and Taylor, B., 2015. Antarctic Ice Sheet response to a long warm interval across Marine Isotope Stage 31: A cross-latitudinal study of iceberg-rafted debris. *Earth and planetary science letters*, 409, pp.109-119.
- Tejavath, C.T., Ashok, K. and Chakraborty, S., 2021. The importance of the orbital parameters for the Indian summer monsoon during the mid-Holocene, as deciphered from atmospheric model experiments. *Frontiers in Earth Science*, 9, p.631310.
- Thadathil, P., Gopalakrishna, V.V., Muraleedharan, P.M., Reddy, G.V., Araligidat, N. and Shenoy, S., 2002. Surface layer temperature inversion in the Bay of Bengal. *Deep Sea Research Part I: Oceanographic Research Papers*, 49, pp.1801-1818.
- Thunell, R.C. and Reynolds, L.A., 1984. Sedimentation of planktonic foraminifera: seasonal changes in species flux in the Panama Basin. *Micropaleontology*, 30, pp.243-262.
- Tiedemann, R., Sarnthein, M. and Shackleton, N.J., 1994. Astronomic timescale for the Pliocene Atlantic  $\delta^{18}\text{O}$  and dust flux records of Ocean Drilling Program Site 659. *Paleoceanography*, 9, pp.619-638.
- Tierney, J.E., Pausata, F.S. and Demenocal, P., 2016. Deglacial Indian monsoon failure and North Atlantic stadials linked by Indian Ocean surface cooling. *Nature Geoscience*, 9, pp.46-50.

- Tripathy, G.R., Singh, S.K. and Ramaswamy, V., 2014. Major and trace element geochemistry of Bay of Bengal sediments: Implications to provenances and their controlling factors. *Palaeogeography, palaeoclimatology, palaeoecology*, 397, pp.20-30.
- Turner, A.G., Inness, P.M. and Slingo, J.M., 2007. The effect of doubled CO<sub>2</sub> and model basic state biases on the monsoon-ENSO system. I: Mean response and interannual variability. *Quarterly Journal of the Royal Meteorological Society: A journal of the atmospheric sciences, applied meteorology and physical oceanography*, 133, pp.1143-1157.
- Ueda, H., Iwai, A., Kuwako, K. and Hori, M.E., 2006. Impact of anthropogenic forcing on the Asian summer monsoon as simulated by eight GCMs. *Geophysical Research Letters*, 33, p. L06703.
- Varkey, M.J., Murty, V.S.N. and Suryanarayana, A., 1996. Physical oceanography of the Bay of Bengal and Andaman Sea. *Oceanography and Marine Biology: An Annual Review*, 34, pp.1-70.
- Wajsowicz, R.C. and Schopf, P.S., 2001. Oceanic influences on the seasonal cycle in evaporation over the Indian Ocean. *Journal of Climate*, 14, pp.1199-1226.
- Webster, P.J., 1986. *The elementary monsoon*. Monsoons, 3.
- Webster, P.J., Magana, V.O., Palmer, T.N., Shukla, J., Tomas, R.A., Yanai, M.U. and Yasunari, T., 1998. Monsoons: Processes, predictability, and the prospects for prediction. *Journal of Geophysical Research: Oceans*, 103, pp.14451-14510.
- Wefer, G., Berger, W.H., Bijma, J. and Fischer, G., 1999. Clues to ocean history: a brief overview of proxies. *Use of proxies in paleoceanography*, pp.1-68.
- Wyrtki, K., Bennett, E.B. and Rochford, D.J., 1971. *Oceanographic atlas of the international Indian Ocean expedition*, 531. Washington, DC: National Science Foundation.
- Xiao, J., Porter, S.C., An, Z., Kumai, H. and Yoshikawa, S., 1995. Grain size of quartz as an indicator of winter monsoon strength on the Loess Plateau of central China during the last 130,000 yr. *Quaternary Research*, 43, pp.22-29.
- Xiao, J. and An, Z., 1999. Three large shifts in East Asian monsoon circulation indicated by loess–paleosol sequences in China and late Cenozoic deposits in Japan. *Palaeogeography, Palaeoclimatology, Palaeoecology*, 154, pp.179-189.
- Yamamoto, M., Sai, H., Chen, M.T. and Zhao, M., 2013. The East Asian winter monsoon variability in response to precession during the past 150 000 yr. *Climate of the Past*, 9, pp.2777-2788.
- Yin, Q.Z. and Guo, Z.T., 2008. Strong summer monsoon during the cool MIS-13. *Climate of the Past*, 4, pp.29-34.
- Zachos, J., Pagani, M., Sloan, L., Thomas, E. and Billups, K., 2001. Trends, rhythms, and aberrations in global climate 65 Ma to present. *Science*, 292, pp.686-693.
- Zahn, R. and Pedersen, T.F., 1991. Late Pleistocene evolution of surface and mid-depth hydrography at the Oman Margin: planktonic and benthic isotope records at Site 724. In *Proceedings of Ocean Drilling Program Scientific Results*, 117, pp. 291-308.



- Zhang, R., Jiang, D., Liu, X. and Tian, Z., 2012. Modeling the climate effects of different subregional uplifts within the Himalaya-Tibetan Plateau on Asian summer monsoon evolution. *Chinese Science Bulletin*, 57, pp.4617-4626.
- Zhang, Y.G. and Liu, X., 2018. Export depth of the TEX86 signal. *Paleoceanography and Paleoclimatology*, 33, pp.666-671.
- Zhang, H., Ait Brahim, Y., Li, H., Zhao, J., Kathayat, G., Tian, Y., Baker, J., Wang, J., Zhang, F., Ning, Y. and Edwards, R.L., 2019. The Asian summer monsoon: Teleconnections and forcing mechanisms—A review from Chinese speleothem  $\delta^{18}\text{O}$  records. *Quaternary*, 2, p.26.
- Ziegler, M., Lourens, L.J., Tuenter, E. and Reichert, G.J., 2010. High Arabian Sea productivity conditions during MIS 13—odd monsoon event or intensified overturning circulation at the end of the Mid-Pleistocene transition?. *Climate of the Past*, 6, pp.63-76.
- Zweng, M.M., Seidov, D., Boyer, T., Locarnini, M., Garcia, H., Mishonov, A., Baranova, O.K., Weathers, K., Paver, C.R. and Smolyar, I., 2019. World ocean atlas 2018, volume 2: Salinity. In: A. Mishonov, Technical Editor. NOAA Atlas NESDIS, 81, pp. 50.